NUREG/CR-3488
Vol. 3

# Idaho Field Experiment 1981

## Volume 3: Comparison of Trajectories, Tracer Concentration Patterns and MESODIF Model Calculations

Prepared by G. E. Start, J. H. Cate, J. F. Sagendorf, G. R. Ackermann, C. R. Dickson, N. H. Nukari, L. G. Thorngren

**Air Resources Laboratories**
**National Oceanic and Atmospheric Administration**

**Prepared for**
**U.S. Nuclear Regulatory Commission**

GPO Printed copy price: $4.50

NUREG/CR-3488
Vol. 3
RB

# Idaho Field Experiment 1981

## Volume 3: Comparison of Trajectories, Tracer Concentration Patterns and MESODIF Model Calculations

Manuscript Completed: February 1985
Date Published: February 1985

Prepared by
G. E. Start, J. H. Cate, J. F. Sagendorf, G. R. Ackermann,
C. R. Dickson, N. H. Nukari, L. S. Thorngren

Air Resources Laboratories
Field Research Division
National Oceanic and Atmospheric Administration
Idaho Falls, ID 83401

**Prepared for**
**Division of Radiation Programs and Earth Sciences**
**Office of Nuclear Regulatory Research**
**U.S. Nuclear Regulatory Commission**
**Washington, D.C. 20555**
**NRC FIN B5690**
**Under Contract No. RES-76-106**

## ABSTRACT

The Idaho Field Experiment is reported in three volumes and supplemented by special contractor reports. Volume I describes the design and goals of the measurement program and the measurement systems utilized during the field program. The measurement systems layouts are described as well.

Volume II lists the data in tabular form or cites the special supplemental reports by other participating contractors. While the primary user file and the data archive are maintained on 9 track/1600 cpi magnetic tapes, listings of the individual values are provided for the user who either cannot utilize the tapes or wishes to preview the data. The accuracies and quality of these data are described.

Volume III contains descriptions of the nine intensive measurement days. General meteorological conditions are described, trajectories and their relationships to analyses of gaseous tracer data are discussed, and overviews of test day cases are presented. Calculations using the ARLFRD MESODIF model are included and related to the gaseous tracer data. Finally, a summary and a list of recommendations are presented.

The 1981 Idaho Field Experiment was conducted in southeast Idaho over the Upper Snake River Plain. Nine test-day case studies were conducted between July 15 and 30, 1981. Releases of $SF_6$ gaseous tracer were made for 8-hour periods from 46 m above ground. Tracer was sampled hourly, for 12 sequential hours, at about 100 locations within an area 24 km square. Also, a single total integrated sample, of about 30 hours duration, was collected at approximately 100 sites within an area 48 by 72 km (using 6 km spacings). Extensive tower profiles of meteorology at the release point were collected. RAWINSONDES, RABALS and PIBALS were collected at 3 to 5 sites. Horizontal, low-altitude winds were monitored using the INEL mesonet. $SF_6$ tracer plume releases were marked with co-located oil fog releases and bi-hourly sequential launches of tetroon pairs. Aerial LIDAR observations of the oil fog plume and airborne samples of $SF_6$ were collected. High-altitude aerial photographs of daytime plumes were also collected.

CONTENTS

List of Figures

List of Figures (cont.)



List of Tables

## ACKNOWLEDGEMENTS

This research was sponsored by the U. S. Nuclear Regulatory Commission (NRC), Office of Nuclear Regulatory Research, under Interagency Agreement No. RES-76-106. It was also sponsored in part by Fast Reactor Safety, Department of Energy (DOE), under Interagency Agreement No. DE-AI02,80ET327246. Data analyses and reporting were supported by the NRC.

Technical direction has been provided by Robert A. Kornasiewicz of the Office of Nuclear Regulatory Research since May 1981.

The Office of Nuclear Regulatory Research, U. S. Nuclear Regulatory Commission, Washington, D. C. recognized the need for and advocated the collection of a comprehensive, high quality data set of gaseous tracer concentration data along with numerous, concurrent meteorological measurements. The ability to exercise and evaluate atmospheric transport and diffusion models is of interest to the NRC. The observations for making those assessments would have been limited without this data set.

Miss Christa Crapo assisted in the initial drafting of parts of the text, gathered together portions of the supporting data, and also assisted in editing of the text.

# I. Introduction

Atmospheric dispersion estimation capabilities are needed for emergency response planning and site characterization. Assessments are required by federal regulation both for site acceptability and emergency planning. The objective of the NRC atmospheric dispersion research program is to provide improved bases for licensing decisions and for development and confirmation of regulations and guides (Abbey, 1982). Emphasis is placed on obtaining high quality data sets, assessment of regulations and evaluation of atmospheric dispersion models. The Idaho Field Study is one of these data collection efforts.

Three fundamental questions arise whenever the potential impact of airborne material is considered, whether the impact be the projected footprint of a model calculation or the footprint of an actual plume. These questions are namely the WHERE, WHEN, and HOW MUCH descriptions of the behavior of that airborne material. Given the entire domain of possible impact, where within that domain will it actually go? When will it get to where it was going? And finally, how great will the concentration be and how long will it remain there?

Volume III of the Idaho Field Experiment (IFX), unlike the previous two volumes, contains descriptions of each individual test and the general conditions surrounding the collection of data. Also included in this volume are plots and contours of various data described in previous volumes. The purpose of the material contained herein is not to evaluate all of the data contained in Volume II of the Idaho Field Experiment, (Start, et al., 1984). Rather, it is to draw out representative data and present it in a manner such that someone desiring to further analyze the data has the information necessary to do so.

The Idaho Field Study was performed on the broad semi-desert upper Snake River Plain in southeastern Idaho. Volume I (Start, et al., 1983) describes the area and climate in detail. The local topographic setting of the plain provides frequent diurnal cycling of the wind from up-valley to down-valley and back. It provides atmospheric conditions typical of many sites with similar temporal cycling of local winds. Flow convergence zones and wind shift lines regularly translate back and forth across the IFX study region and provide special opportunities for measurements during these conditions. Figure I-1 depicts the IFX test area as it relates to local topography. Figure I-2 shows the locations of sampling sites for the large grid and their relation to the larger regional setting.

To provide some answers, perhaps stimulate additional questions, and demonstrate areas of needed increased understanding, the MESODIF model has been run on the IFX data set. Model domains were chosen which encompass the tracer sampling grids along with a border of additional outer grid points to handle recirculation should it occur. Model receptor points correspond to sampling points on the grid. Because the model uses a full grid but the samplers do not comprise a

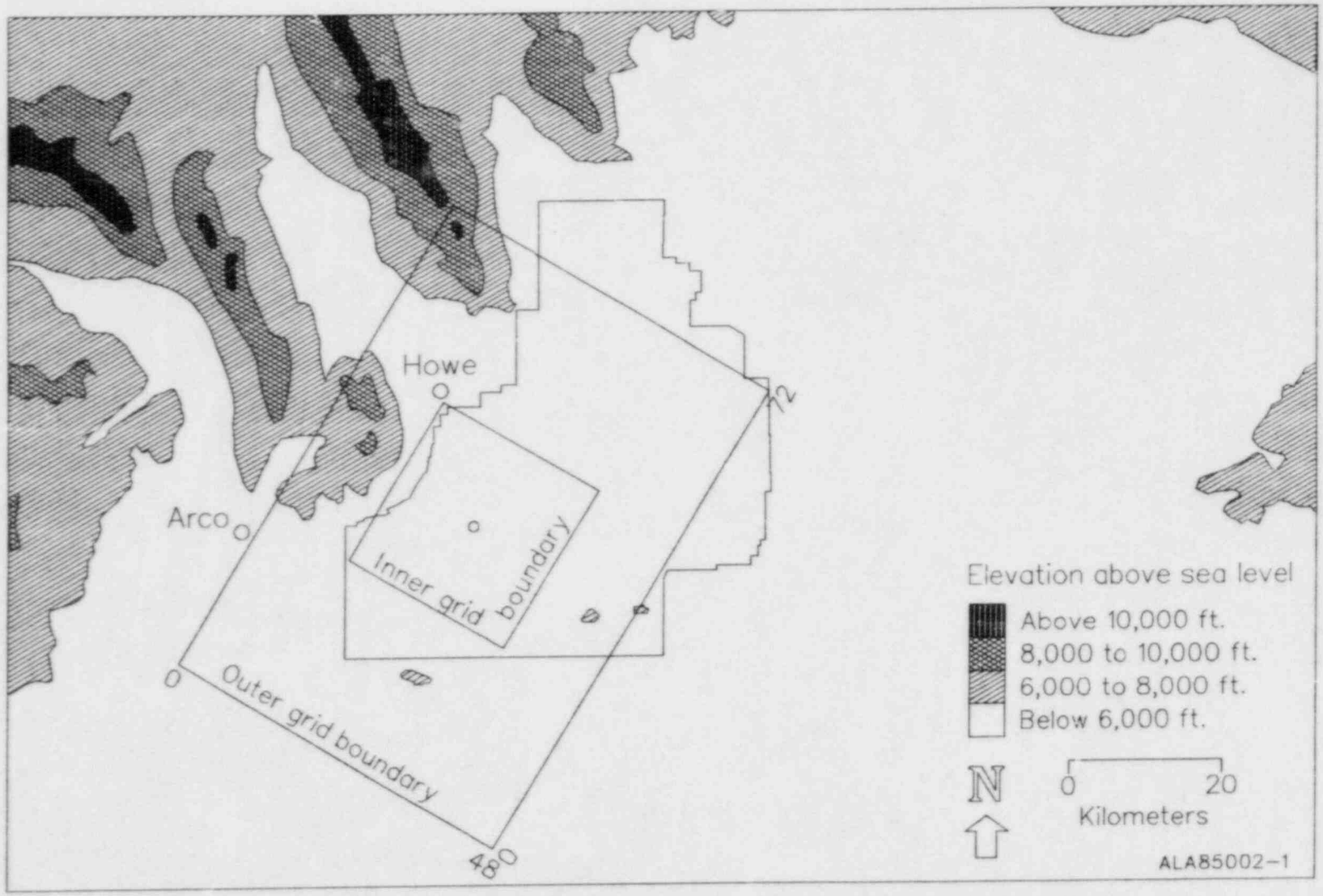


Figure I-1. Location of IFX grid in relationship to terrain features

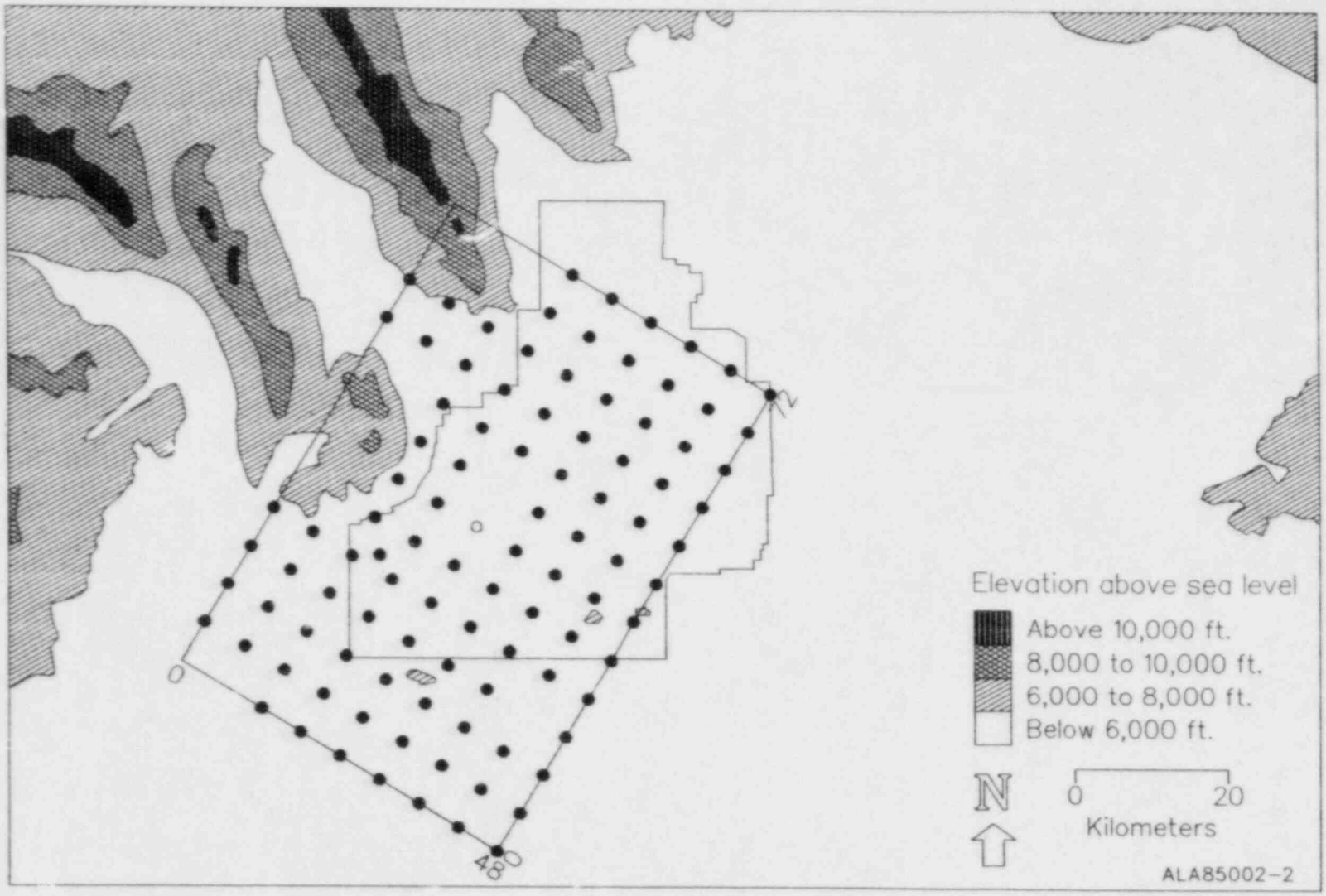


Figure I-2. Map of the IFX large grid sampling locations

full field, an interpolation method was used to map the sample data onto a uniform grid which fully correspondes to the model field. Characteristics of the MESODIF model are discussed in Chapter II.

Chapter III presents a broad overview of the meteorological conditions which occurred on the test dates. A brief discussion of synoptic weather conditions and the local winds is also presented.

With this background, illustrations and discussions in Chapter IV examine where the IFX plumes were transported. Several impact zones are defined, based on the climatological characteristics of the area. Tetroon and MESODIF trajectories are used for comparisons with the tracer data to determine hit and miss regions in a qualitative sense.

The questions of "how much" impact are examined quantitatively in Chapter V. Considerations presented include how much total area in the sampling grid is impacted, and how much did the model predict? What caused the difference? How well did the model do?

The findings and interpretations are summarized in Chapter VI. Chapter VII presents recommendations for other analyses, alternate modeling efforts, and suggests supplemental topics for further study.

## II. MESODIF model

The mesoscale diffusion model, MESODIF (Start and Wendell, 1974), was originally developed as a diagnostic research tool. Many modular changes have been made to the model since then to explore various problems and to evaluate model sensitivities. One of these formulations was used with the meteorological data sets of the IFX test series. Model outputs were generated to simulate the trajectory and tracer concentration data from the nine tests. Computations were made for both the inner small grid with 1 km spacing and the large outer grid with 6 km spacing. Before proceeding with discussions of the results of these computations and the IFX data comparisons, a description of MESODIF and the manner in which it was used is appropriate.

The MESODIF model uses a trajectory calculation method based upon time and space variable winds. The trajectory advection technique has been coupled with a plume diffusion scheme which assumes Gaussian mass distribution functions for plume segments. These plume segments which in turn represent the continuous plume are simulated by a series of puffs. These puffs are required to have circular symmetry in the horizontal plane, mostly as a convienence during computations.

Vertical diffusive spreading of the puffs is limited by a capping lid which can vary from hour to hour. This limiting of vertical plume growth follows the suggestion of Turner (1970). During the daytime, the capping lid corresponds to the height of the top of the turbulent planetary boundary. At night, the lower limit of this depth of plume mixing is held at 200 m or greater. Within a specific hour, this lid is assumed to be a constant height above ground-level throughout the entire modeled area. Atmospheric stability category is determined from the rate of change of temperature with height according to the NRC guidelines (NRC Regulatory Guide 1.111). Within a particular hour, the stability category is held constant, but it may change from hour to hour.

The spacial distribution of the modeled plume effluents are represented by the superpositioning of the ensemble of puffs. The temporal behavior of the modeled airborne material is represented by the successive updated locations of the puff ensemble. At each ensuing time step, new puff center locations are determined. Then, based upon the current stability category, the distance moved during the latest temporal displacement, and the previous size of the puff element in question, individual calculations are made of the incremental growth of puff dimensions, puff center concentration, and radial extent of puff influence. Finally, the contributions of each puff at the points of the receptor array are determined and accumulated. In this manner, the temporal behavior of airborne material is modeled. Examples of these model characteristics have been presented and discussed by Start and Wendell (1974).

Several changes have been made in the original model. The model has been restructured into three major program modules, instead of one

large program. The first module builds a disk file of the model control parameters. These parameters are utilized as needed by the other modules.

The second module builds the meteorological parameter data file. Wind data from the INEL MESONET are mapped onto an evenly spaced cartesian grid. A weighting technique based upon the inverse square of distance from the locations of wind measurements is used (Wendell, 1972). A new mapping of winds is made each six minutes from the MESONET data. Stability, mixing depth, and a unit source term are also placed in the wind parameter data file. The stability category descriptions for this series of model runs were obtained from the Grid III tower temperature profiles. They were updated every hour along with the mixing depths. Mixing depths were determined from the climatological data base for the INEL. A diurnal hour-by-hour variation of mixing depth is derived from the climatological daily maximum and the assumed 200m minimum. An hourly variation is formulated to parallel the rate of heating of the layer of air near 2m above the ground. Observations by the SRI aircraft lidar during midday, tests 1 and 2, found oil fog plume elements up to heights of 3000 meters above ground-level. These maximum plume heights agree with the expected July maximum climatological value of 3000m used for these model runs.

The final module of the MESODIF model, when coupled with the control parameters and meteorological data from programs 1 and 2, performs the advection and diffusion calculations. Changes were made in portions of this code to facilitate the use of 6 minute instead of hourly meteorological data along with hourly updates of the stability and mixing depth. MESODIF uses empirical, stability-stratified curves of horizontal and vertical diffusion indices, sigma-y and sigma-z, developed from measurements at the INEL. These curves are for the desert-like climate which exists at the INEL (Yanskey, et al., 1966). They represent spreading of releases from 15 to 60 minute duration.

MESODIF computations were initiated at a modeling time corresponding to the onset of tracer release. Each modeling run simulated an eight hour plume genesis during the 80 initial six-minute time steps of the computation. Ten puffs or plume segments were used to simulate each hour of tracer release. Computations were continued until all modeled plume material was advected out of the computational grid. A release height of 45 meters was used. The IFX grid was rotated 29 degrees clockwise from North. The small grid computations were made using a 29 by 29 receptor array with the source located at (15,15). The large grid computations were made using a 13 by 17 receptor array and source at (7,9). Grid intervals were 1 km (.6214 miles) and 6 km (3.7282 miles), respectively.

## III. General weather during IFX test cases

Intensive measurements were conducted during nine periods in July, 1981. These dates and times are shown in Table III-1. In general, the IFX weather and temperature patterns were very typical of July, with high pressure over the area most of the time. With the exception of an upper-level trough during test 6, no strong, large-scale weather pattern significantly influenced testing periods during the IFX test series. The daily regional wind circulations were generally dominated by local conditions. These conditions were influenced by the diurnal heating cycle, thunderstorms, and by the formation, dissipation, and movement of the local scale wind convergence zone.

Table III-1. Dates and times (MDT) of 1981 Idaho Field Experiment.

| Test No. | Date | Julian Date | Tracer Release Time |
|---|---|---|---|
| 1 | July 15 | 196 | 1100-1900 |
| 2 | July 17 | 198 | 1100-1900 |
| 3 | July 18-19 | 199-200 | 2300-0700 |
| 4 | July 20-21 | 201-202 | 2300-0700 |
| 5 | July 23 | 204 | 0500-1300 |
| 6 | July 25-26 | 206-207 | 1700-0100 |
| 7 | July 27 | 208 | 1300-2100 |
| 8 | July 29 | 210 | 0500-1300 |
| 9 | July 30-31 | 211-212 | 1700-0100 |

The following general meteorological conditions occurred during the nine IFX intensive measurement periods. The descriptions are grouped by test number.

Test 1: (Release time: 1100-1900 MDT) July 15

A 500 mb trough developed off the West Coast. Over Idaho a minor ridge gave way to westerly flow with a weak trough over southern British Columbia. A weak frontal system was over northern Utah.

Some convective activity developed during late afternoon over the mountains. No precipitation fell in the test area.

An up-valley wind with low speeds occurred in the early afternoon, continued into early evening, and shifted to a down-valley drainage flow later that night.

Test 2: (Release time: 1100-1900 MDT) July 17

A weak southwesterly flow at upper levels continued over Idaho, with a weak low over northwestern Washington. A surface low pressure and frontal system developed in southwestern Idaho and intensified during the test period.

No precipitation fell in the IFX grid area. Shower activity occurred over the mountains to the North and East. Clearing skies developed as the test progressed.

Winds were light, up-valley early in the afternoon. Wind directions shifted and became down-valley at the end of the tracer release.

Test 3: (Release time: 2300-0700 MDT) July 18-19

The high pressure ridge over the Pacific Ocean west of southern California moved eastward and the 500 mb gradient over southern Idaho strengthened. At the surface, weak low pressure to the south over northern Utah and weak high pressure to the north aided the down-valley direction of the nocturnal drainage winds.

Some convective activity developed during the late morning over the mountains to the north of the area. No precipitation occurred in the study area.

Generally clear skies and drainage winds existed during the night. The flow shifted to up-valley shortly after sunrise.

Test 4: (Release time: 2300-0700 MDT) July 20-21

The 500 mb height contour gradient continued to strengthen over Idaho. During the test, 500 mb wind speeds were between 40 and 50 knots. The surface pressure gradient was slightly weaker than during test 3.

No precipitation fell in the test area.

The down-valley flow which continued throughout the tracer release period weakened during the morning. Up-valley winds returned with daytime heating.

Test 5: (Release time: 0500-1300 MDT) July 23

The 500 mb pattern changed very little from the flow during test 4. The previously predominant "Four Corners" high had now moved eastward into Texas.

Fair skies prevailed over the study area for this test. No precipitation occurred in the area.

Test 5: (Release time: 0500-1300 MDT) (continued)

The down-valley winds were established as the test commenced. These winds weakened and became up-valley during the late morning. Nocturnal drainage winds again set in after midnight.

Test 6: (Release time: 1700-0100 MDT) July 25-26

A significant 500 mb trough moved over Idaho from the West Coast during this test period. High pressure over Texas at 500 mb moved to the southeastern United States. A large surface high pressure tracked across southern Canada. Weak low pressure developed over Nevada.

Considerable convective activity developed over southeast Idaho near the test site. This activity moved through the test area during the early test hours with skies clearing before midnight. One one-hundredth of an inch of precipitation was recorded at the Central Facilities Area.

A strong down-valley gradient became established at the beginning of the test and persisted throughout the test period.

Test 7: (Release time: 1300-2100 MDT) July 27

The upper flow turned from northwesterly to a westerly zonal flow pattern during further eastward progression and weakening of the trough which had affected the area during test 6. By the end of the period a weak trough was again becoming established along the west coast of Canada. An upper-level thermal trough established itself over Idaho. High pressure over the north central United States continued to move eastward and the pressure gradient weakened throughout the test.

There was no precipitation nor significant cloud cover in the study region during this test.

Up-valley winds were established with the onset of daytime heating. This wind flow existed at the time of test initiation and continued throughout the afternoon into early evening; then the wind direction became more southerly. A south wind continued and the airflow from the vicinity of the tracer release point was channeled up Little Lost River Valley beyond Howe. After midnight, a weak, low-level, down-valley drainage wind developed.

Test 8: (Release time: 0500-1300 MDT) July 29

An upper-level trough off the West Coast moved slowly inland, keeping Idaho under a southwesterly flow aloft. The 500mb upper level high also remained over the southeastern United States. Only weak surface pressure gradients existed across the United States.

Skies were fair over the southeastern Idaho during this test. No precipitation occurred within the study region.

A steady down-valley wind was established and continued throughout the morning. By midday after daytime heating had progressed, the winds diminished, reversed, and southwest up-valley winds set in for the remainder of the day.

Test 9: (Release time: 1700-0100 MDT) July 30-31

A weakening upper level trough continued to move eastward across southern Canada, all the while becoming more distant from Idaho . There was very little change in the upper flow pattern from the test 8 conditions, particularly over southern Idaho. The 500 mb high remained over the southern United States. A cold front approaching the Pacific Northwest lost strength as it moved inland. A second weak frontal system continued to move eastward through Wyoming as surface high pressure built over southern Canada and the northern Rockies. This high pressure brought clear skies to southeast Idaho for this test.

No precipitation occurred over the study area.

Southwesterly up-valley winds occurred during the tracer release and diminished late that night as weak down-valley winds developed. With the on-set of heating the next day, winds rapidly turned to the southwest and strengthened in speed throughout the day.

## IV. Comparisons of trajectories and transport characteristics

An important element in the description of the behavior of airborne effluents in the atmosphere is the path along which the plume mass is transported. A number of descriptive measurements were made during IFX and have been listed and discussed (Start, et al, 1984, chapters 2-6). A verification of the effective arrival of the gaseous tracer at ground-level and aerial receptors is given by the tracer sampling data in chapters 8-13 (ibid. ). The $SF_6$ tracer sampling data for the ground-level receptors ( ibid., chapters 8 and 9 ) are available to evaluate the performance of plume transport descriptions. Trajectories of tetroons and trajectories calculated from the MESONET array of tower mounted wind sensors (refered to as MESONET trajectories) will be compared to one another and to the area(s) of plume impact as shown by the $SF_6$ tracer samples.

For the discussion of similarities and differences between the various indicators of transport and trajectories, six characteristic regions within the IFX study setting are defined. These six regions are shown in Figure IV-1. Regions 1 and 2 are to the southwest and northeast of the Grid III release point along the paths of the two prevailing wind directions. Transport into and beyond these zones would be expected with typical July diurnal wind patterns. Region 3 is more to the south of the GRID III release point and trajectories into this zone are less frequent. Region 4 represents the zone to the east and southeast of GRID III into which direct plume transport would be infrequent. Region 5 denotes a zone near the mountains at the edge of the study area and northwest of GRID III. Winds from the southeast are relatively infrequent at the Grid III tower. Trajectories into this zone may occur during episodes of channeled or recirculated transport, or during early daylight hours when initial heating occurs on the eastward facing mountain slopes. Region 6 represents a zone of canyon wind transport. The Howe and Little Lost wind observations provide measurements of these airflows.

Qualitative assessments may be made by comparing which of these zones were impacted by the $SF_6$ tracer and whether or not the MESODIF calculated trajectories or the tetroon flights indicated transport into the same regions. Figures IV-2 through IV-10 illustrate the tetroon trajectories for tests 1 through 9, respectively; corresponding sets of trajectories derived from MESONET winds (one trajectory for each pair of tetroons) are shown in Figures IV-11 through IV-19. These MESONET (MESODIF) trajectories are based upon winds mostly observed 15m above ground. Tetroons were frequently at heights greater than 100m above ground-level. During periods of strongly stable thermal stratification in the lower atmosphere some of the MESONET trajectories should be expected to differ substantially from the tetroon trajectories.

For the large grid transport comparisons within the IFX measurement domain shown in Figure IV-1, the 30-hour $SF_6$ gaseous tracer concentrations from Volume II were used. A qualitative summary of the transport phenomena and tracer sampling results, region by region, are shown in Table IV-1. Concentration values less than 15 parts per

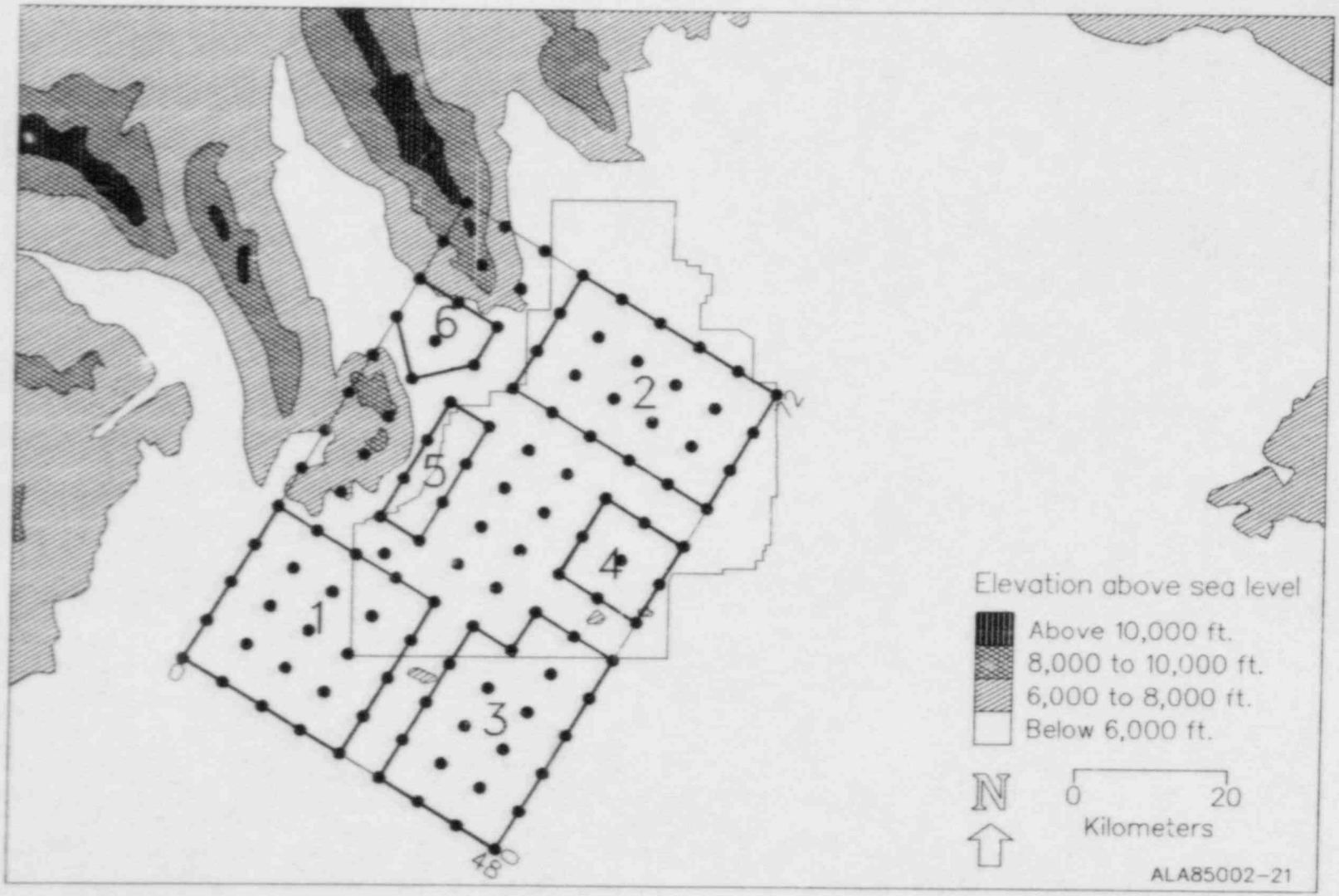


Figure IV-1. Characteristic zones over the IFX study area

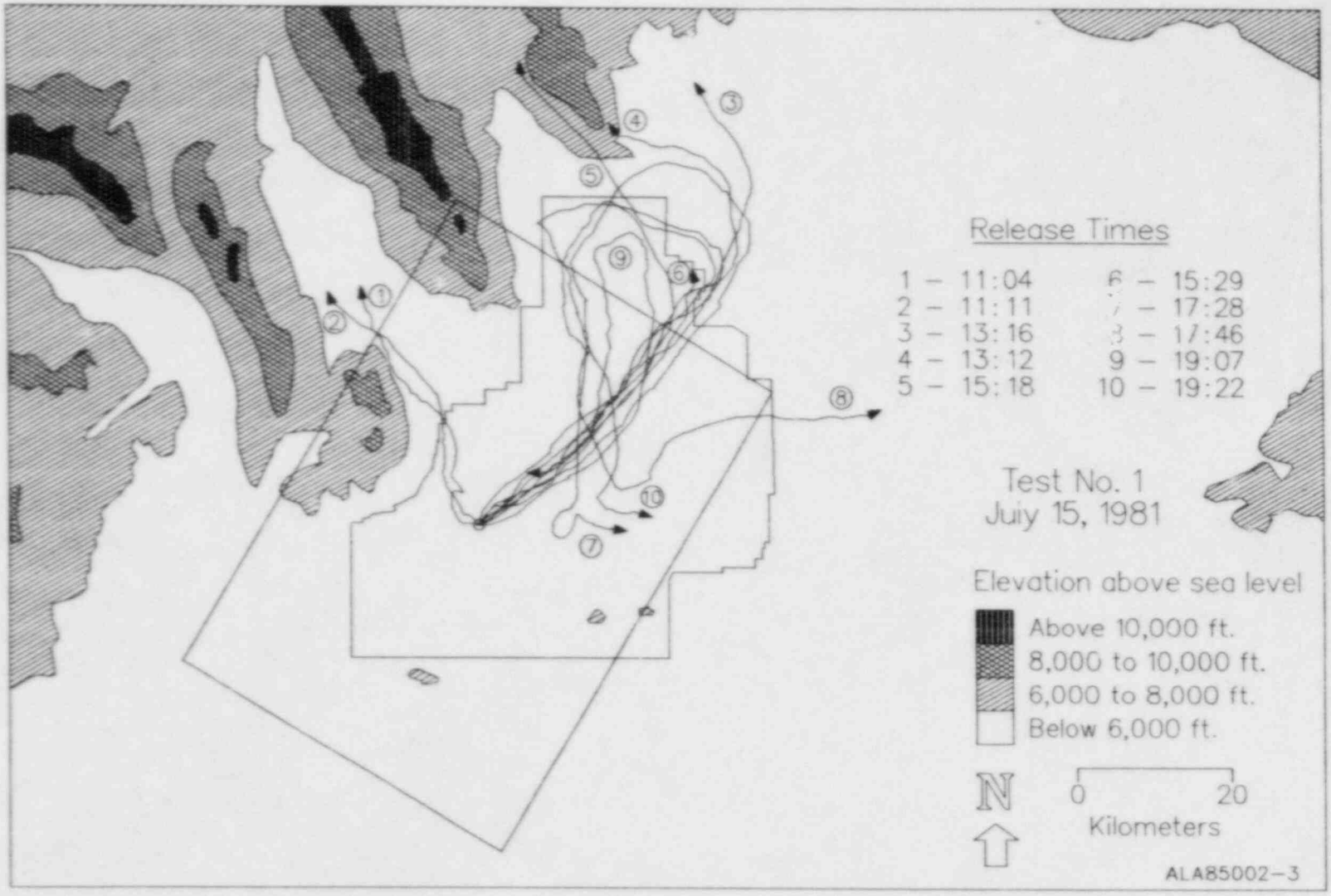


Figure IV-2. Tetroon trajectories Test 1, 15 July 1981

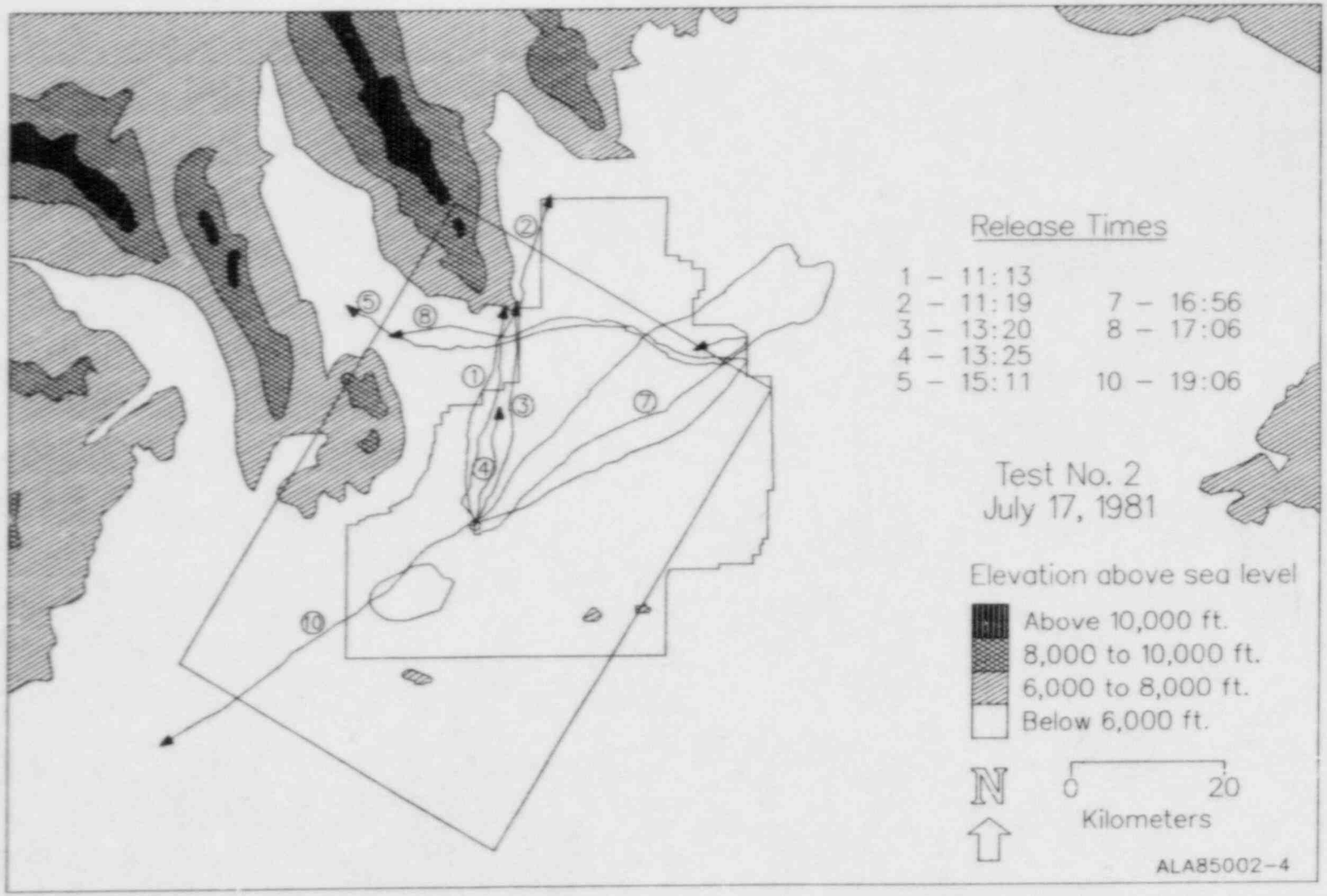


Figure IV-3. Tetroon trajectories Test 2, 17 July 1981

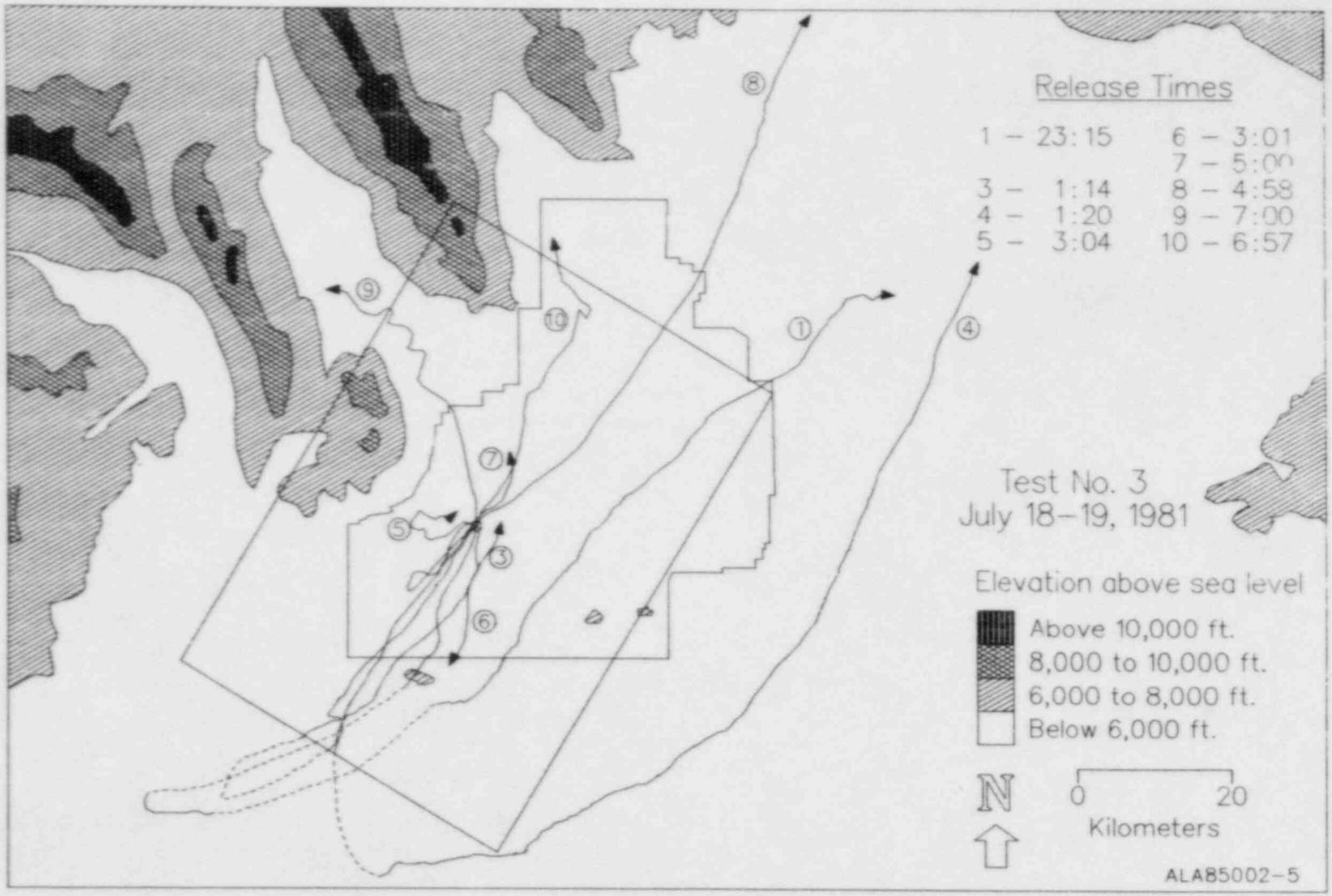


Figure IV-4. Tetroon trajectories, Test 3, 18-19 July 1981

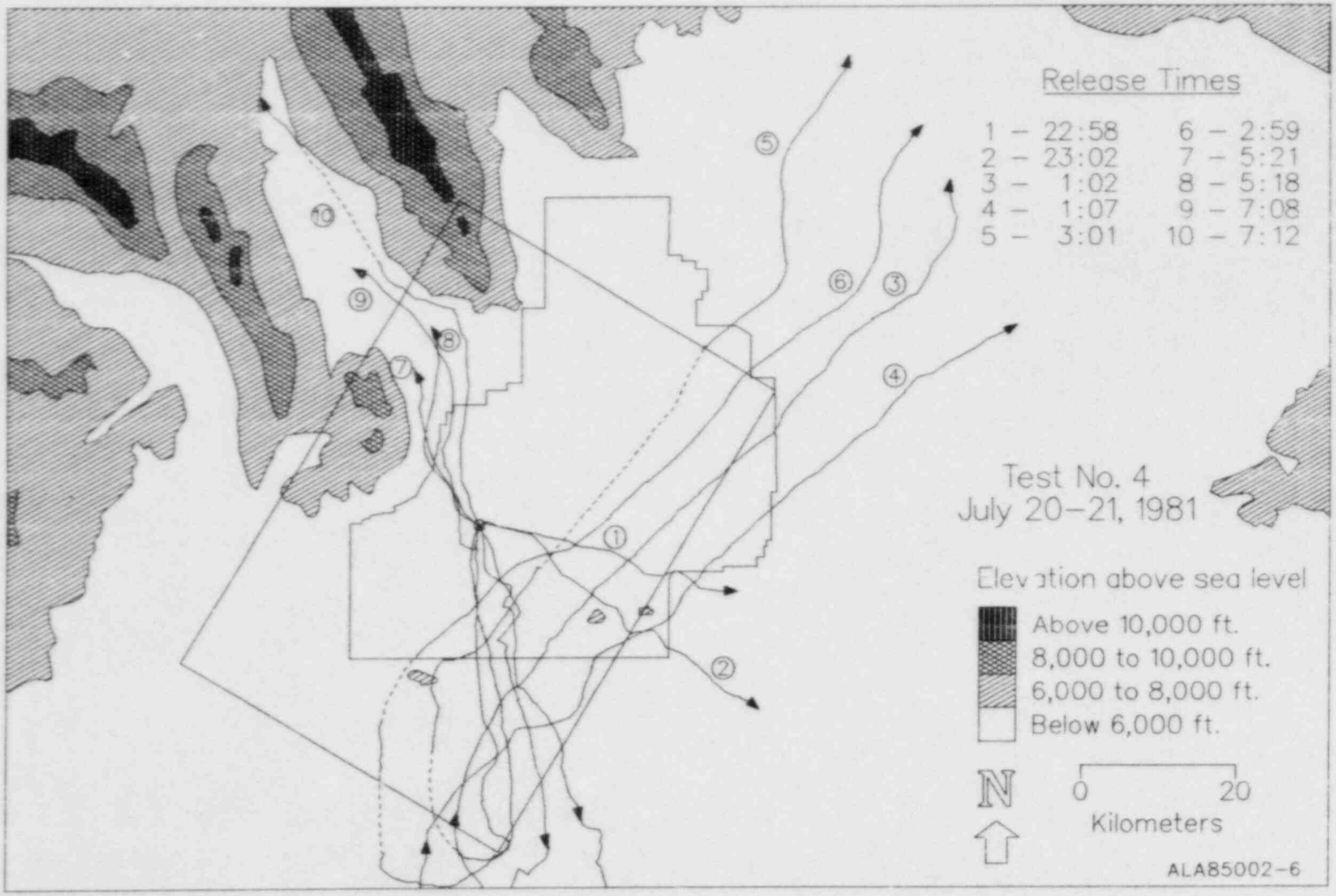


Figure IV-5. Tetroon trajectories, Test 4, 20-21 July 1981

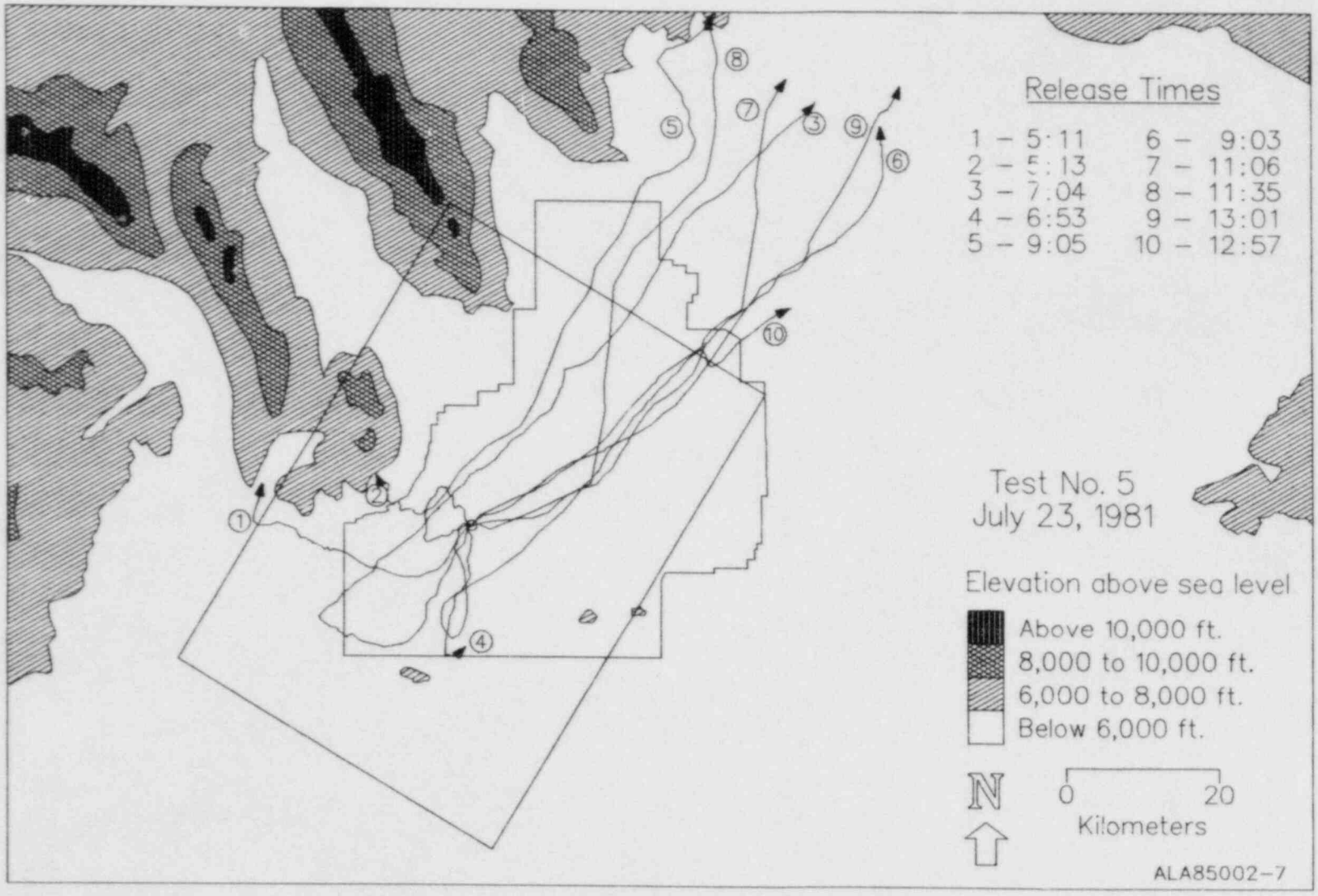


Figure IV-6. Tetroon trajectories, Test 5, 23 July 1981

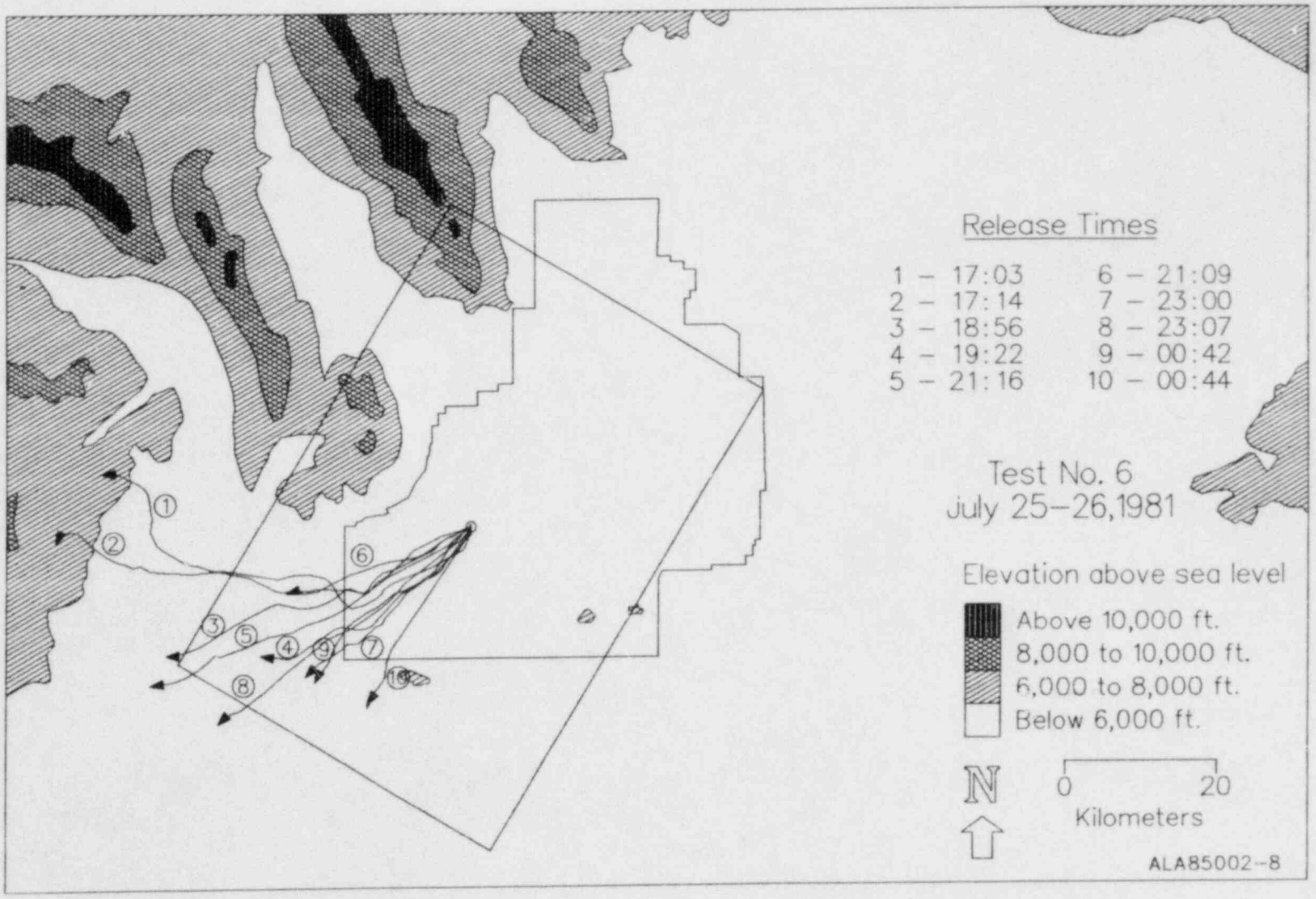


Figure IV-7. Tetroon trajectories, Test 6, 25-26 July, 1981

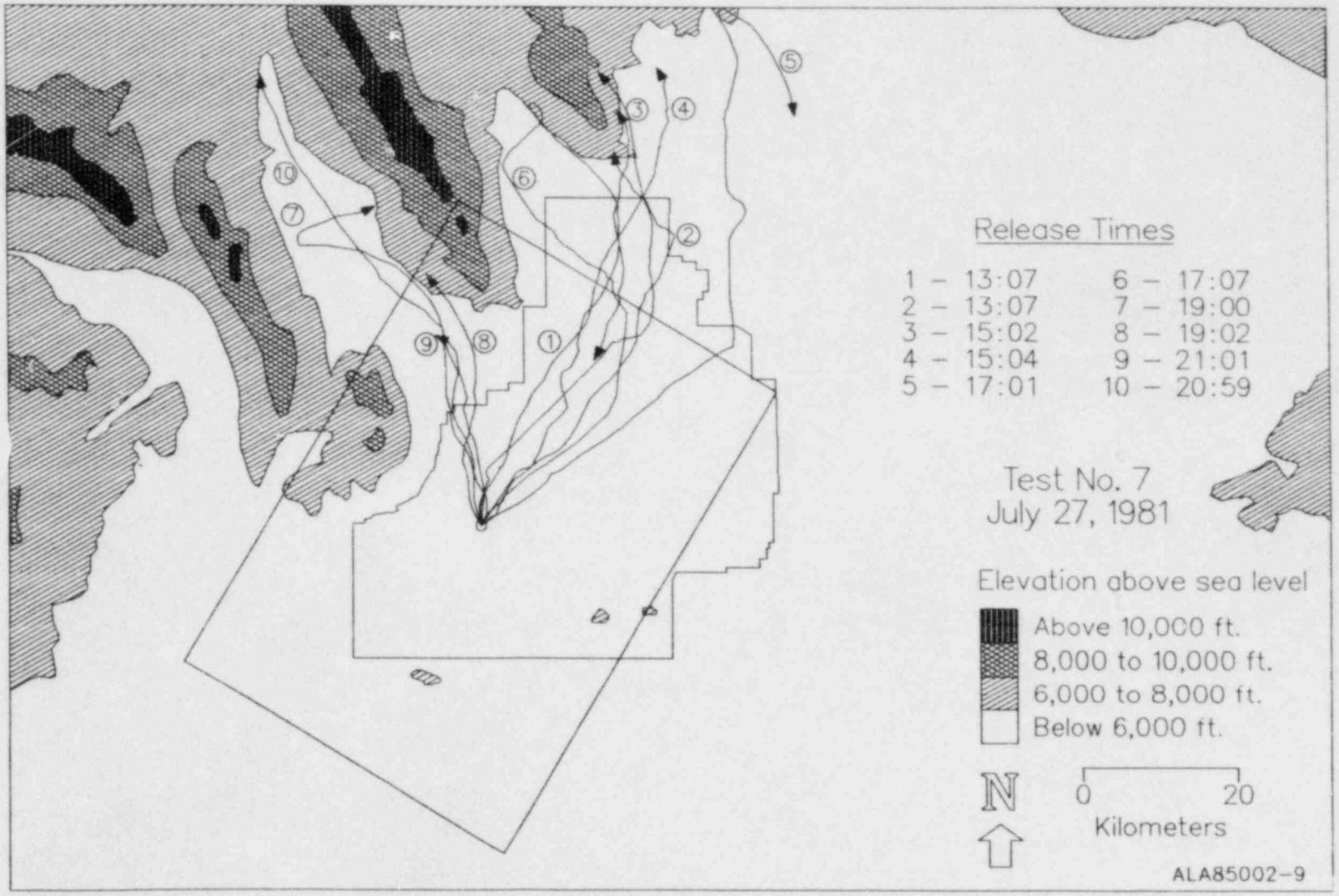


Figure IV-8. Tetroon trajectories, Test 7, 27 July 1981

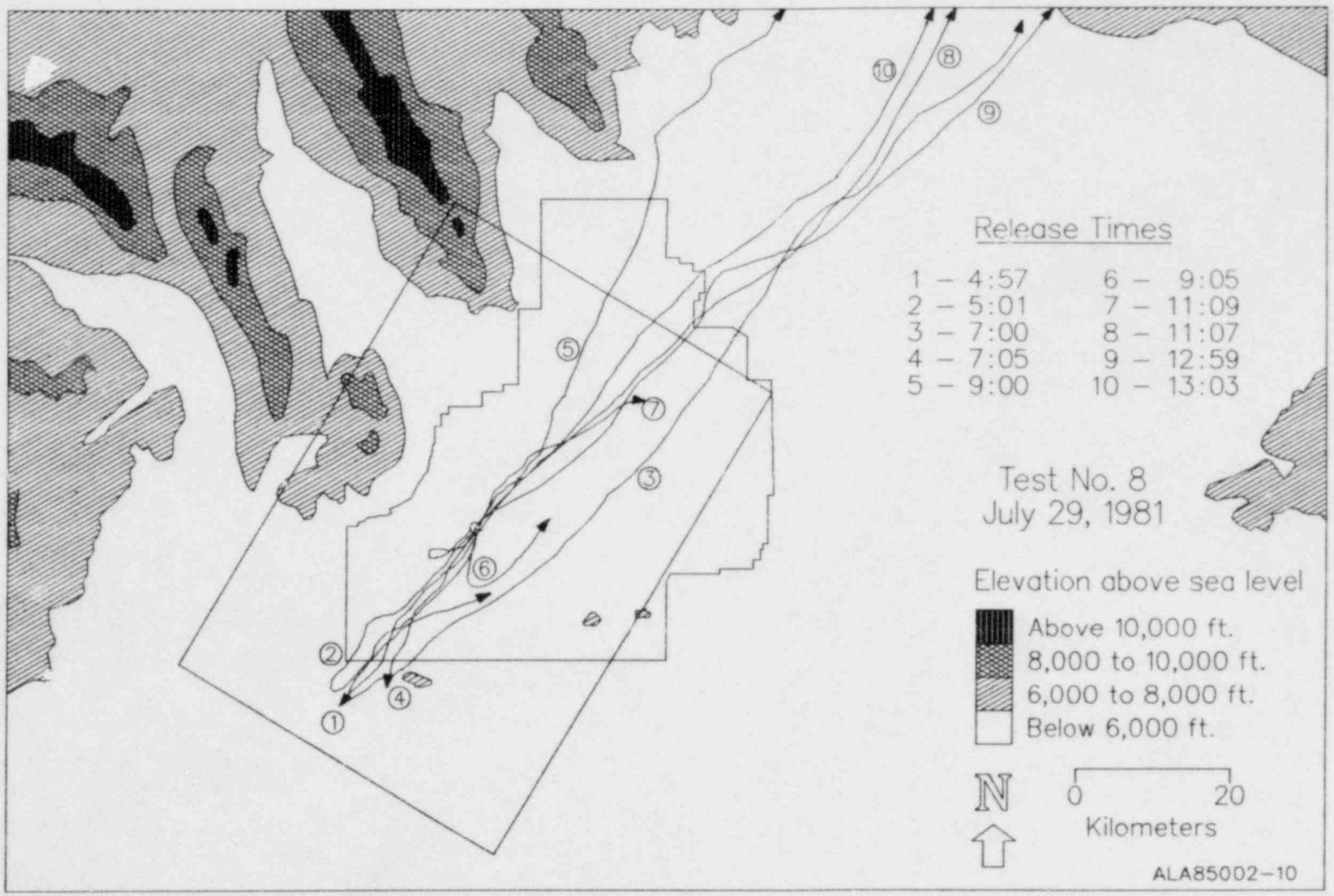


Figure IV-9. Tetroon trajectories, Test 8, 29 July 1981

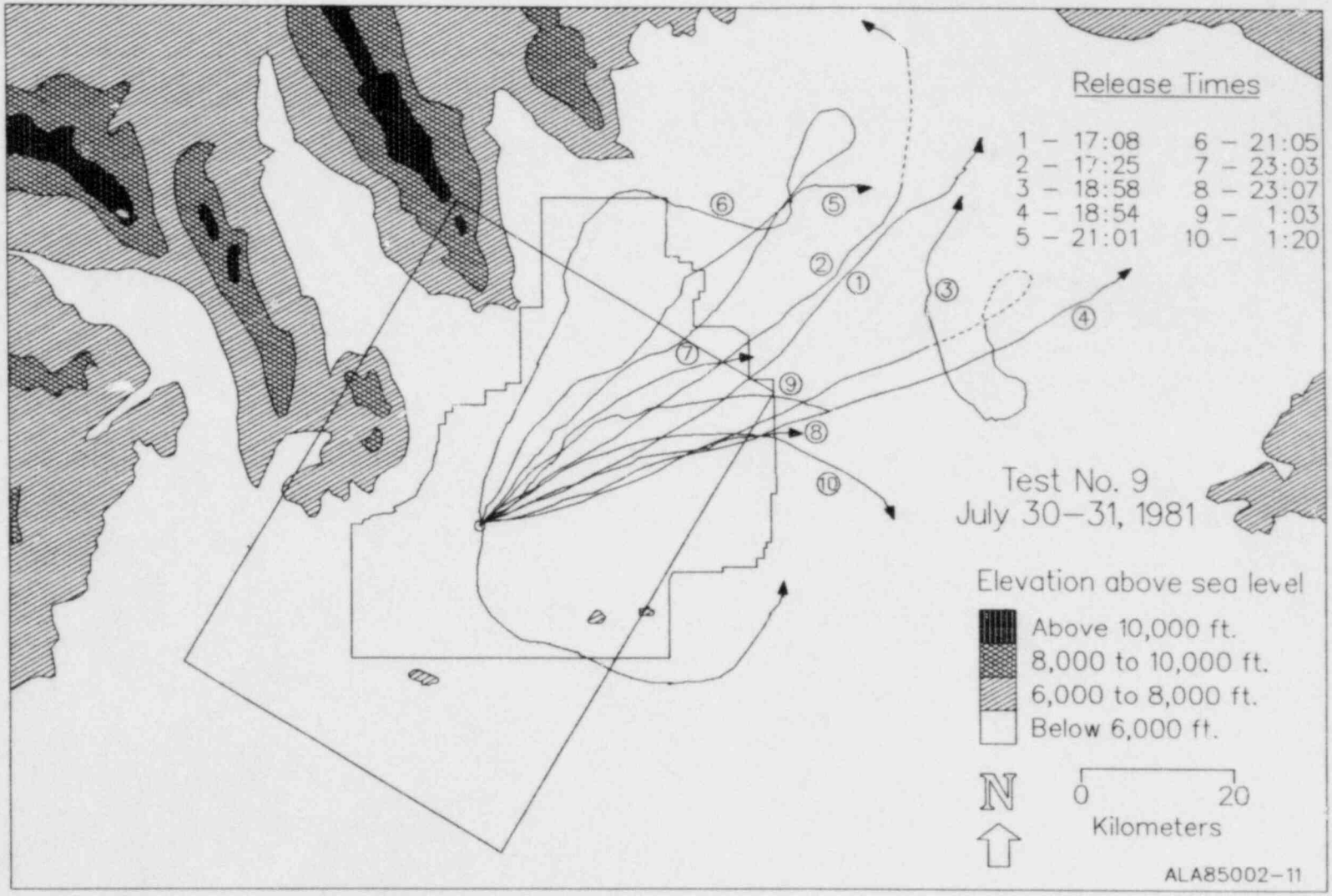


Figure IV-10. Tetroon trajectories, Test 9, 30-31 July 1981

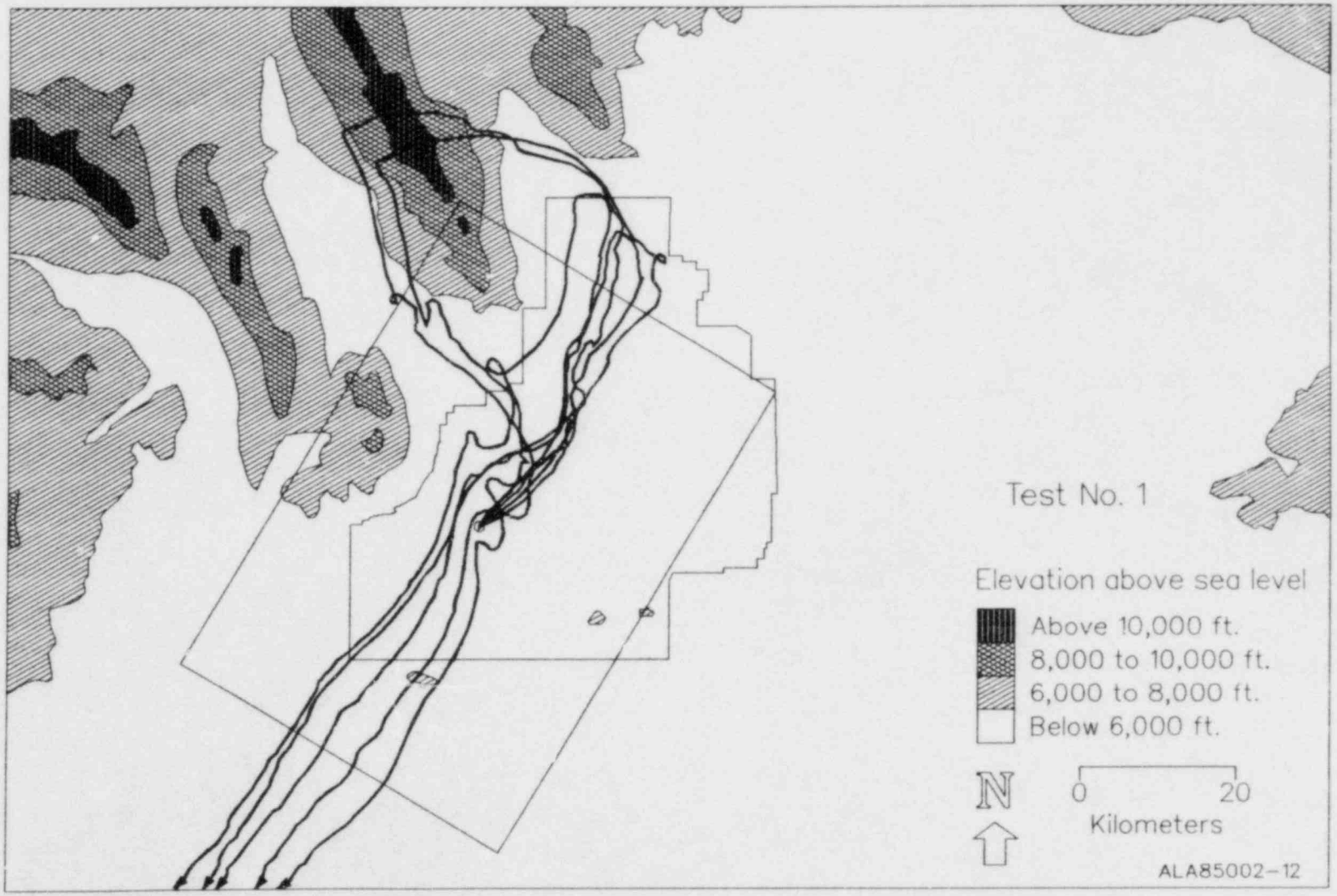


Figure IV-11. MESODIF trajectories, Test 1

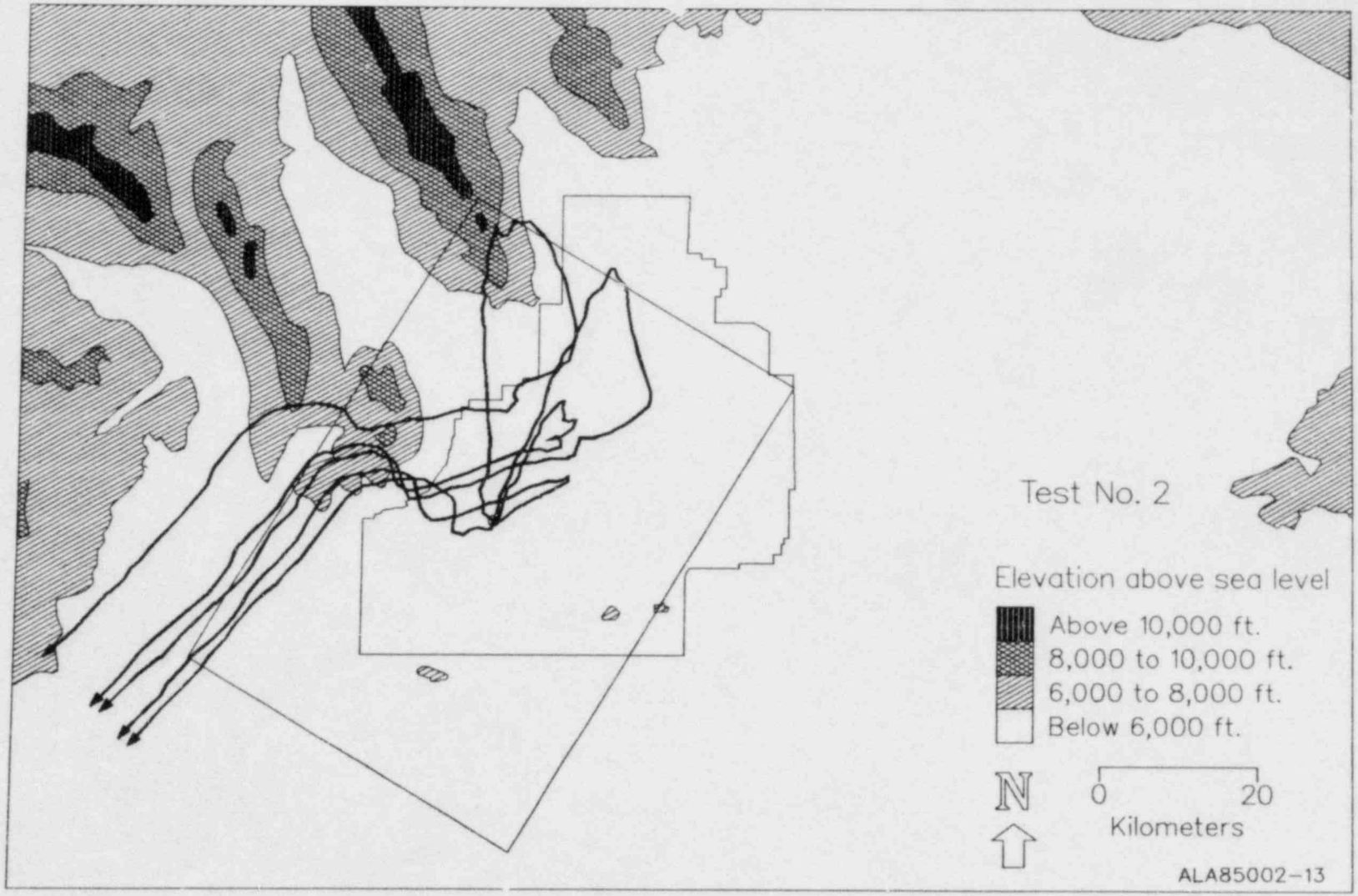


Figure IV-12. MESODIF trajectories, Test 2

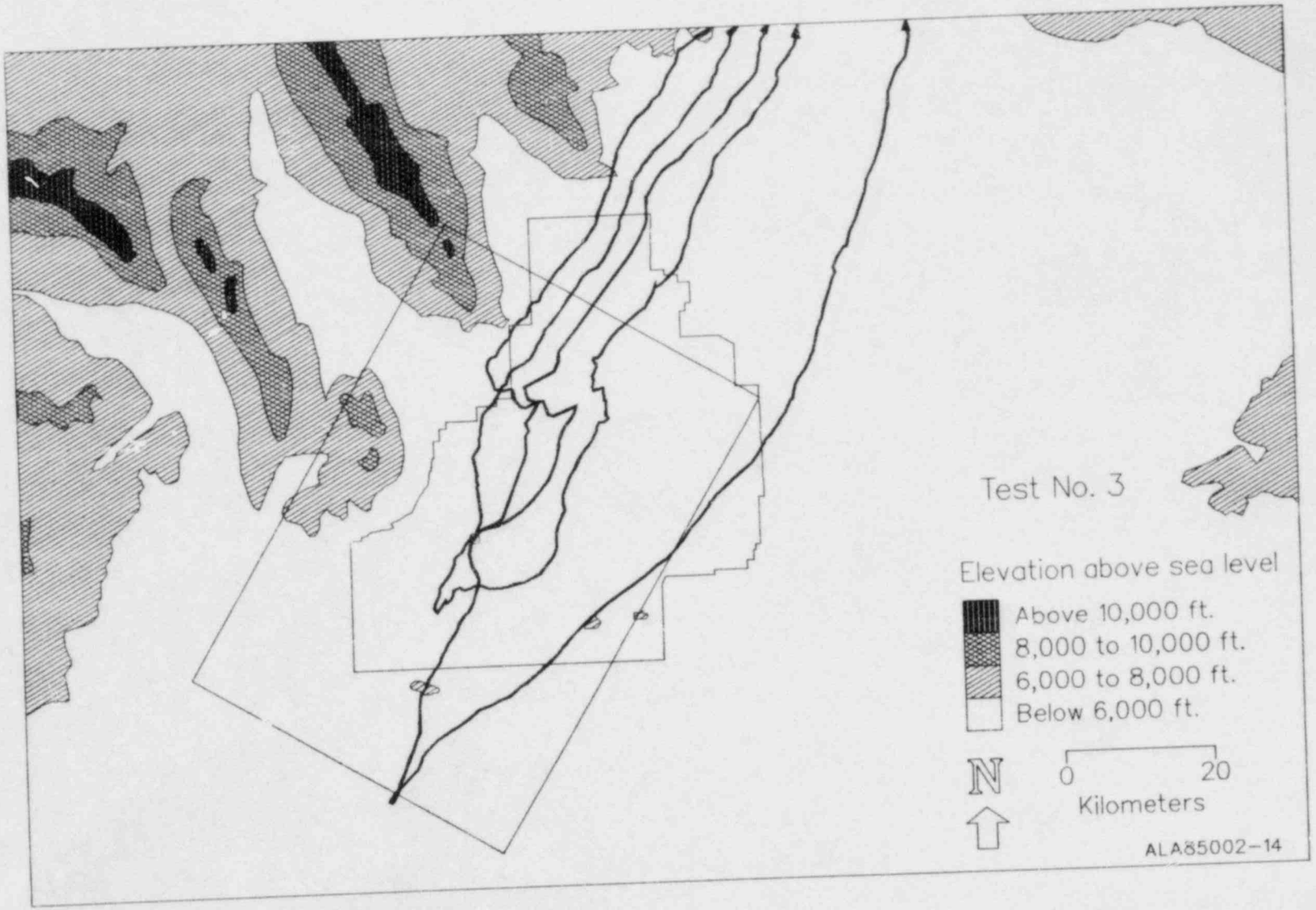


Figure IV-13. MESODIF trajectories, Test 3

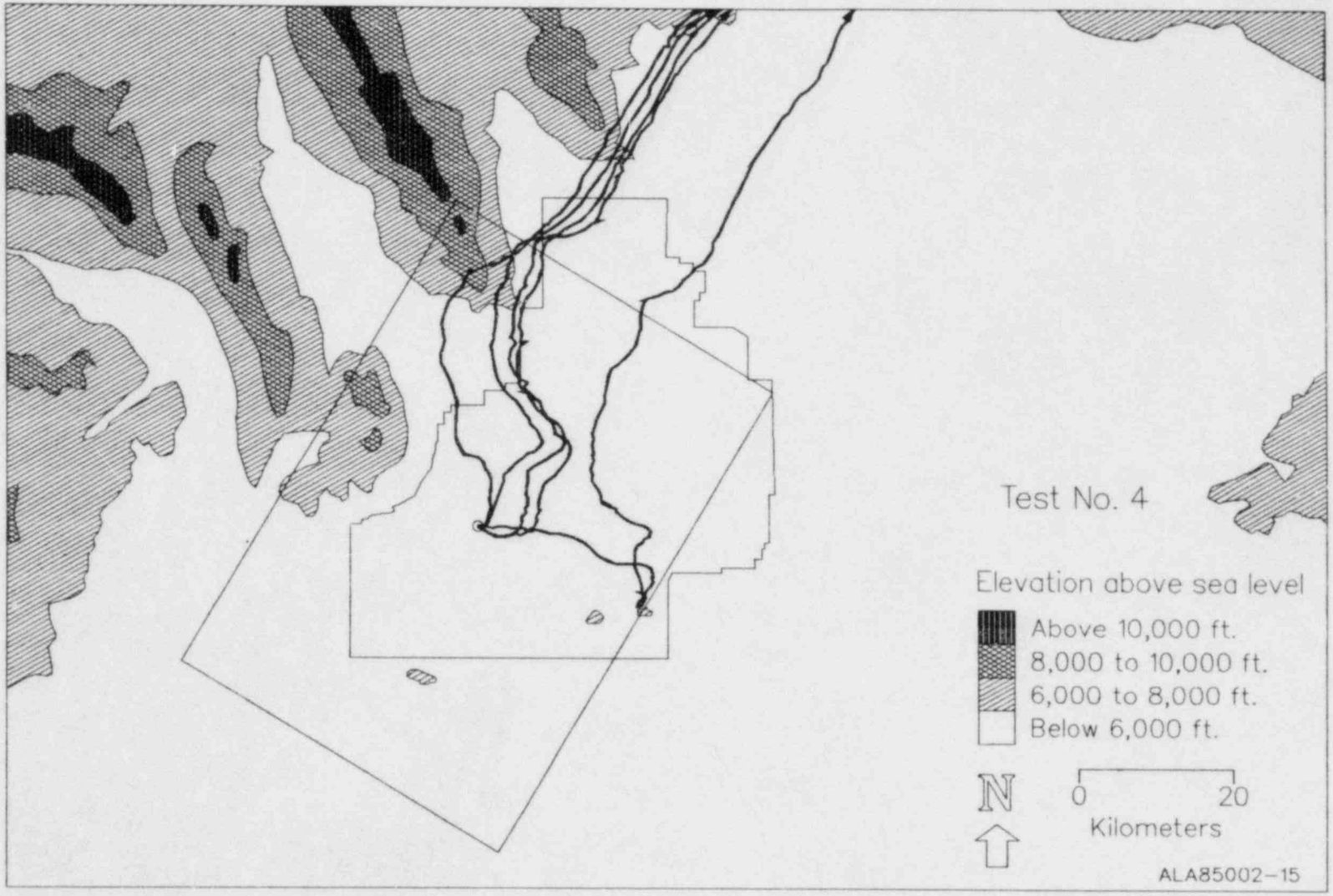


Figure IV-14. MESODIF trajectories, Test 4

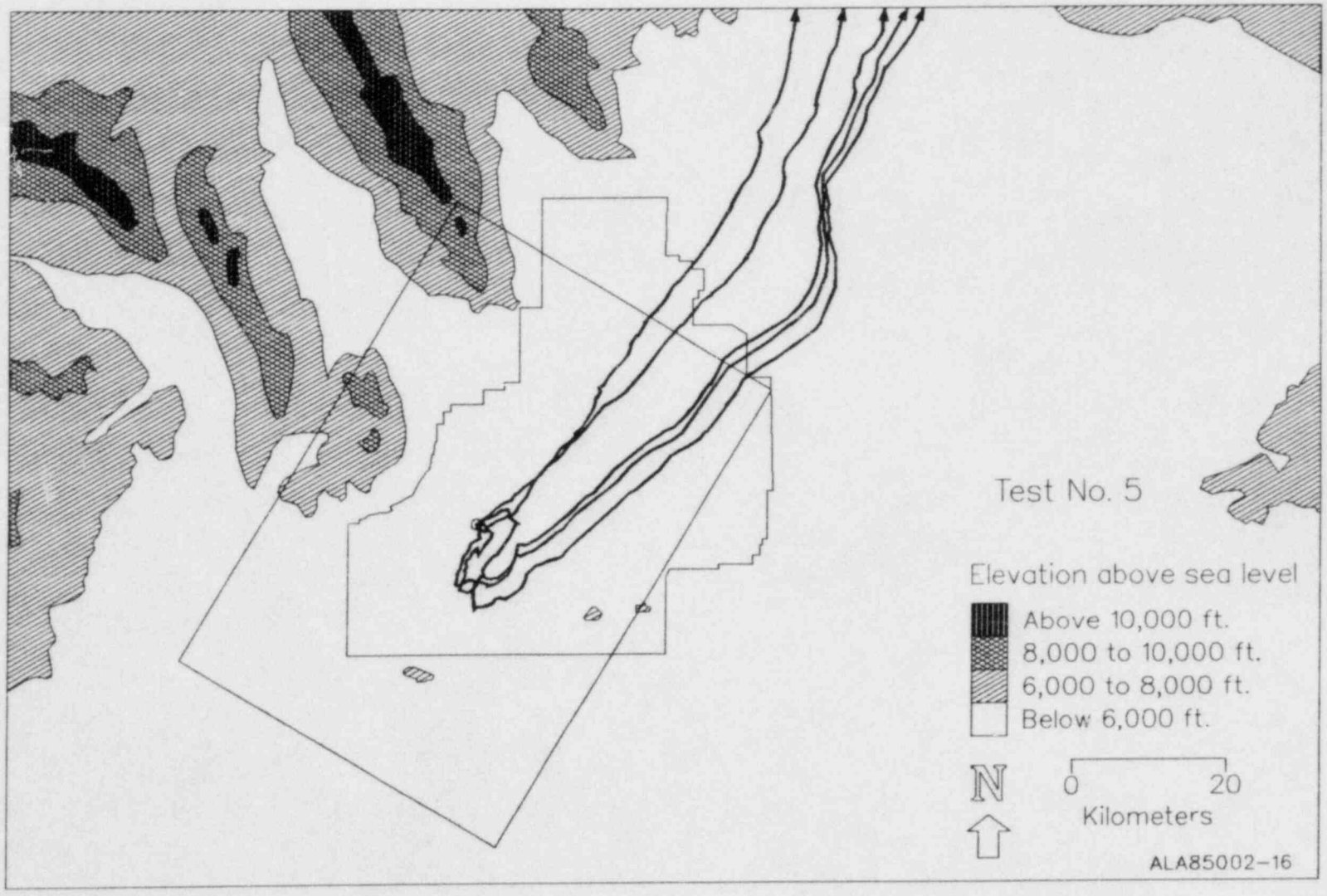


Figure IV-15. MESODIF trajectories, Test 5

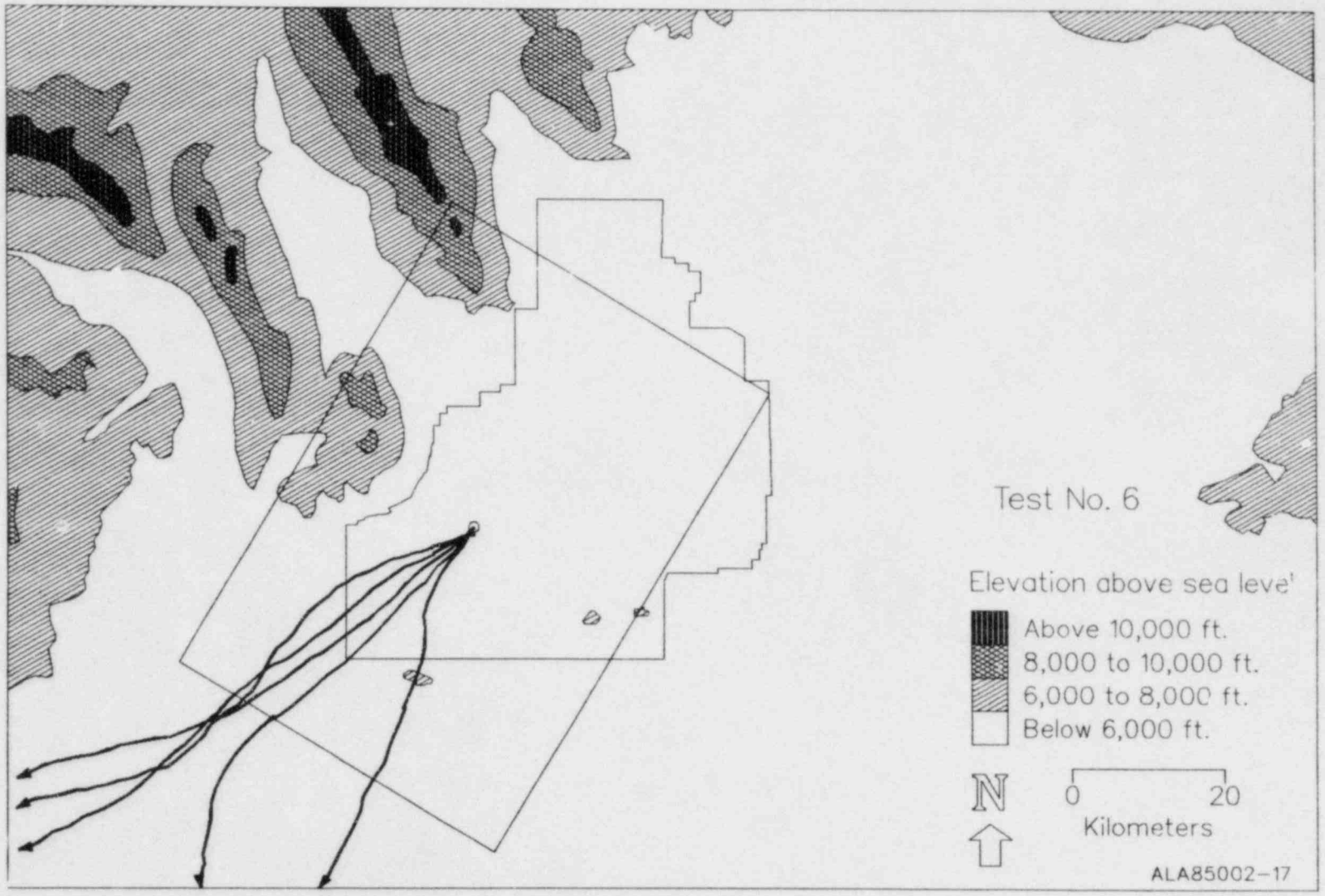


Figure IV-16. MESODIF trajectories, Test 6

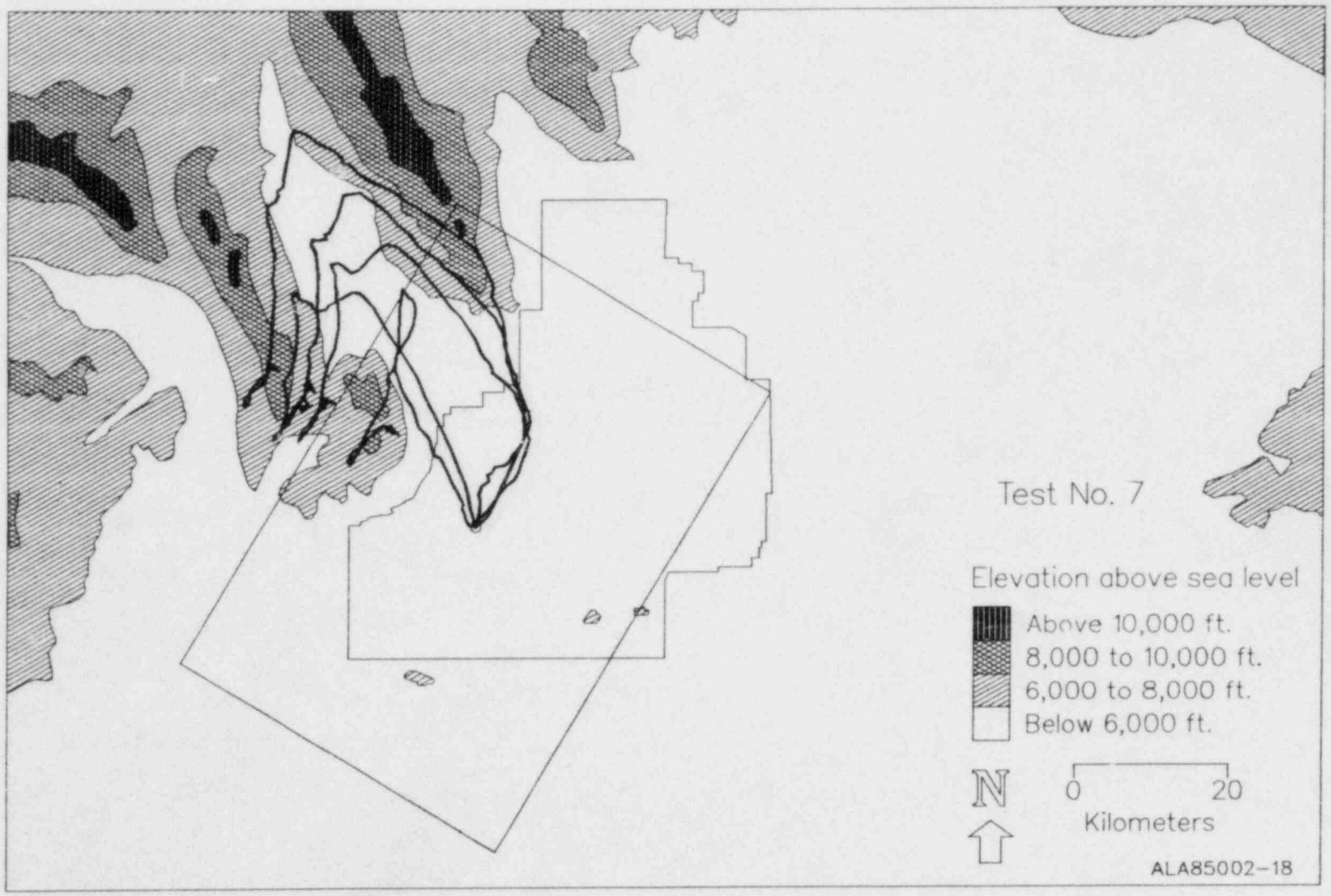


Figure IV-17. MESODIF trajectories, Test 7

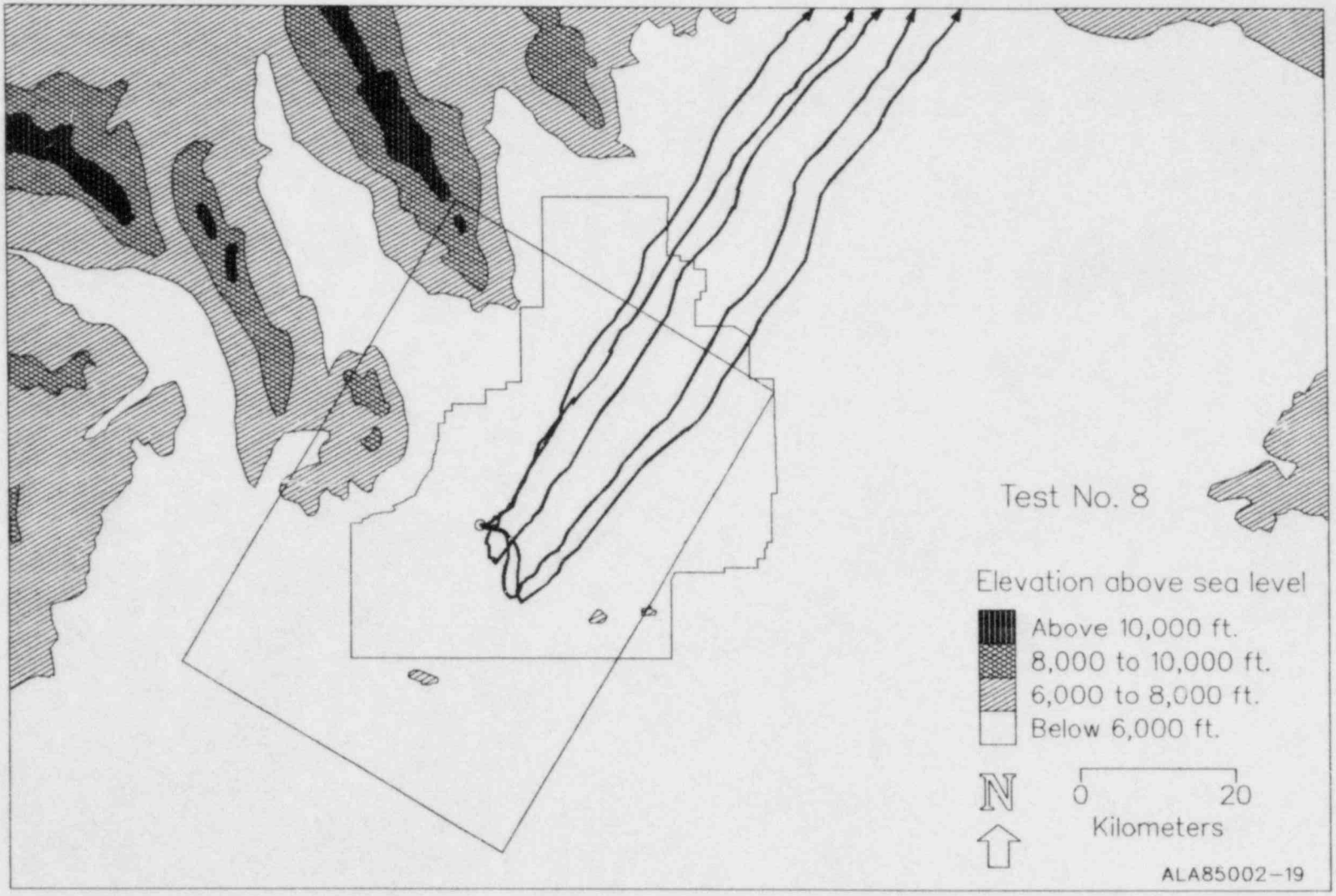


Figure IV-18. MESODIF trajectories, Test 8

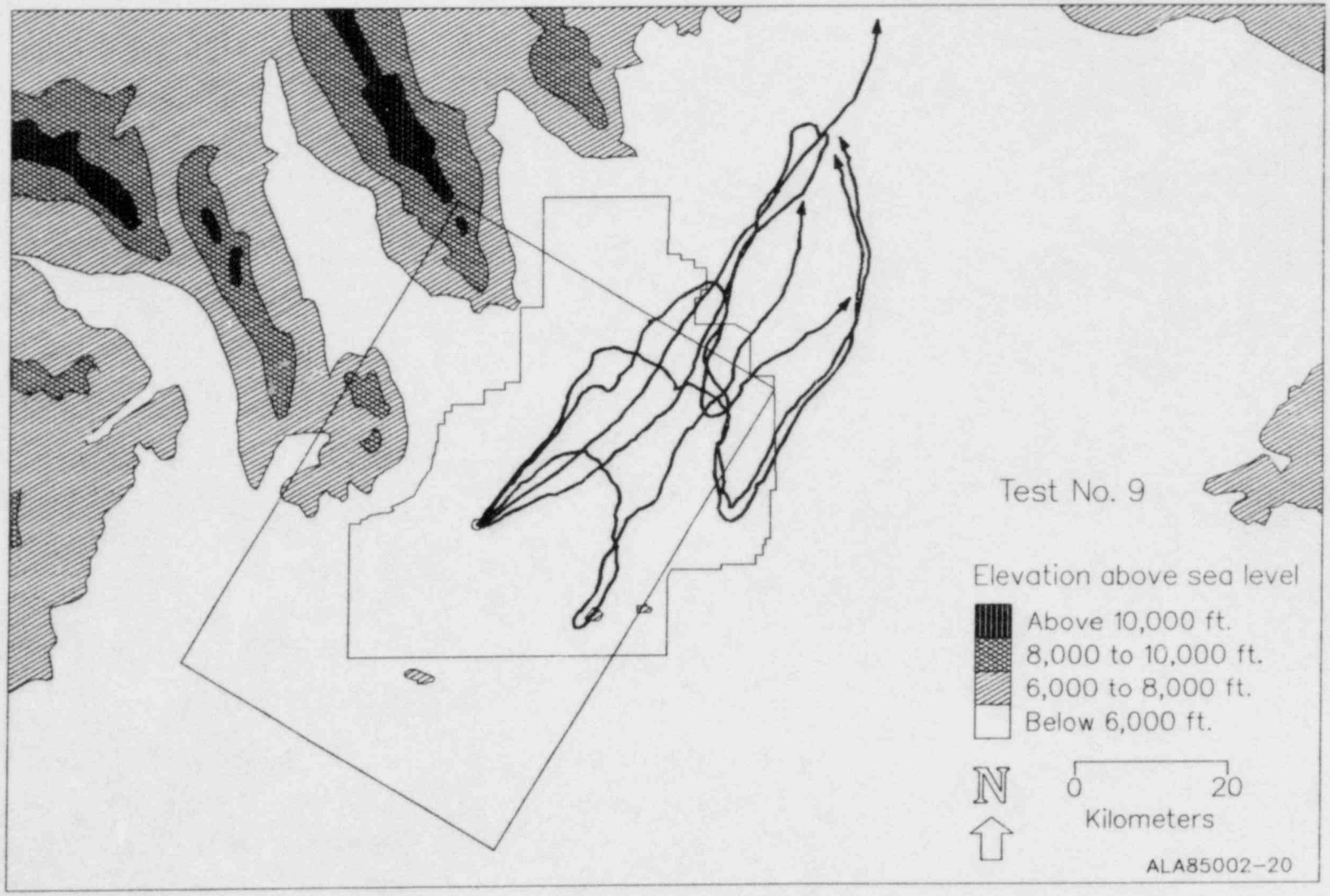


Figure IV-19. MESODIF trajectories, Test 9

trillion (volume to volume) were considered to be null values (values less than 6 times the detection threshold). The occurrence in each zone of tracer detection, tetroon overflights, and advection calculated using MESONET winds are summarized below. A successful verification means that the presence (or absence) of $SF_6$ tracer is accounted for by either MESONET or tetroon trajectories traveling into (avoiding) the zone. The "hits" and "misses" for each of these three phenomena are shown by zone number versus test number. A hit (or positive occurrence) is shown by the symbol " x " and a " - " shows a miss. The comparisons and discussions of these events will follow.

Table IV-1. $SF_6$ impactions, tetroon overflights, and MESONET wind advections.

| | | IFX Test Number | | | | | | | | |
|---|---|---|---|---|---|---|---|---|---|---|
| Zone | Marker | 1 | 2 | 3 | 4 | 5 | 6 | 7 | 8 | 9 |
| 1 | $SF_6$ | x | x | x | x | x | x | - | x | - |
| | MESONET | x | x | x | - | x | x | - | - | - |
| | Tetroon | - | x | x | - | x | x | - | x | - |
| 2 | $SF_6$ | x | x | x | x | - | - | x | - | x |
| | MESONET | x | x | x | x | x | - | - | x | x |
| | Tetroon | x | x | x | x | x | - | x | x | x |
| 3 | $SF_6$ | x | x | x | x | x | - | x | x | - |
| | MESONET | - | - | x | - | x | - | - | x | x |
| | Tetroon | - | - | x | x | - | - | - | - | - |
| 4 | $SF_6$ | x | - | x | x | - | - | - | - | x |
| | MESONET | x | - | x | x | - | - | - | - | x |
| | Tetroon | - | - | x | x | - | - | - | - | x |
| 5 | $SF_6$ | - | x | x | x | x | x | x | - | - |
| | MESONET | - | x | - | - | - | - | x | - | - |
| | Tetroon | - | - | - | - | x | - | - | - | - |
| 6 | $SF_6$ | x | x | x | x | - | - | x | - | - |
| | MESONET | x | x | - | x | - | - | x | - | - |
| | Tetroon | x | x | x | x | - | - | x | - | - |

A simple but direct means of comparing observed versus calculated hits and misses is the 2 x 2 contingency table. For the case of perfect agreement between calculated and observed behaviors all entries would be either in the upper left or lower right cells of the table, i.e., along the principal diagonal. Several of these tables follow to assist in the understanding of results given in Table IV-1. Within these tables H denotes hit and M denotes miss. A number of stratified comparisons are presented to provide insight into systematic behaviors of calculated versus modeled transport indicators. The first comparison is made by test number, with separate tables for each test.

Test 1

| | | Observed H | Observed M | |
|---|---|---|---|---|
| Calc | H | 4 | 0 | 4 |
| | M | 1 | 1 | 2 |
| | | 5 | 1 | 6 |

Test 2

| | | Observed H | Observed M | |
|---|---|---|---|---|
| Calc | H | 4 | 0 | 4 |
| | M | 1 | 1 | 2 |
| | | 5 | 1 | 6 |

Test 3

| | | Observed H | Observed M | |
|---|---|---|---|---|
| Calc | H | 5 | 0 | 5 |
| | M | 1 | 0 | 1 |
| | | 6 | 0 | 6 |

Test 4

| | | Observed H | Observed M | |
|---|---|---|---|---|
| Calc | H | 4 | 0 | 4 |
| | M | 2 | 0 | 2 |
| | | 6 | 0 | 6 |

Test 5

| | | Observed H | Observed M | |
|---|---|---|---|---|
| Calc | H | 3 | 1 | 4 |
| | M | 0 | 2 | 2 |
| | | 3 | 3 | 6 |

Test 6

| | | Observed H | Observed M | |
|---|---|---|---|---|
| Calc | H | 1 | 0 | 1 |
| | M | 1 | 4 | 5 |
| | | 2 | 4 | 6 |

Test 7

| | | Observed H | Observed M | |
|---|---|---|---|---|
| Calc | H | 3 | 0 | 3 |
| | M | 0 | 3 | 3 |
| | | 3 | 3 | 6 |

Test 8

| | | Observed H | Observed M | |
|---|---|---|---|---|
| Calc | H | 2 | 1 | 3 |
| | M | 0 | 3 | 3 |
| | | 2 | 4 | 6 |

Test 9

| | | Observed H | Observed M | |
|---|---|---|---|---|
| Calc | H | 2 | 1 | 3 |
| | M | 0 | 3 | 3 |
| | | 2 | 4 | 6 |

Typically, transport into 5 of the 6 zones is correct for each test, and one zone is incorrect. (i.e., 5 of 6 values in the contingency table lie along the primary diagonal and one value is off this diagonal.) There seems to be no basic difference for individual tests. For the 54 possible test-zone assessments, about 83% of the transport comparisons are correctly specified by either or both of the tetroon or calculated MESONET trajectories. Timing of plume arrival is not addressed; that topic is deferred for additional study.

A second stratification of transport comparisons is provided by the following set of six tables. The tables list results for the individual six zones; all zones have good results. Zones 3 and 5 may have slightly poorer correspondence between calculations and tracer observations, but the data set is small and the differences are not considered significant.

Zone 1

| | | Observed H | Observed M | |
|---|---|---|---|---|
| Calc | H | 6 | 0 | 6 |
| | M | 1 | 2 | 3 |
| | | 7 | 2 | 9 |

Zone 2

| | | Observed H | Observed M | |
|---|---|---|---|---|
| Calc | H | 6 | 2 | 8 |
| | M | 0 | 1 | 1 |
| | | 6 | 3 | 9 |

Zone 3

| | | Observed H | Observed M | |
|---|---|---|---|---|
| Calc | H | 4 | 1 | 5 |
| | M | 2 | 2 | 4 |
| | | 6 | 3 | 9 |

Zone 4

| | | Observed H | Observed M | |
|---|---|---|---|---|
| Calc | H | 4 | 0 | 4 |
| | M | 0 | 5 | 5 |
| | | 4 | 5 | 9 |

Zone 5

| | | Observed H | Observed M | |
|---|---|---|---|---|
| Calc | H | 3 | 0 | 3 |
| | M | 3 | 3 | 6 |
| | | 6 | 3 | 9 |

Zone 6

| | | Observed H | Observed M | |
|---|---|---|---|---|
| Calc | H | 5 | 0 | 5 |
| | M | 0 | 4 | 4 |
| | | 5 | 4 | 9 |

All zones (all data pooled together) have correct transport for 45 of 54 comparisons, or about 83% correct. Zones 1 and 2 are grouped together since they contain the areas downwind along the directions of the prevailing winds. The remaining zones, 3 through 6, were also grouped. They represent the "off-axis" transport and were not along either of the prevailing wind directions. These last two tables (for zones 3-6 and 1-2 ) both show 83% correspondence between calculations and observations. For the "off-axis" data set (zones 3-6), five of the six errors occur in zones 3 and 5. Zones 3 and 5 are the regions most expected to be influenced by recirculated segments of tracer plumes.

All Zones

| | | Observed | | |
|---|---|---|---|---|
| | | H | M | |
| Calc | H | 28 | 3 | 31 |
| | M | 6 | 17 | 23 |
| | | 34 | 20 | 54 |

Zone 3-6

| | | Observed | | |
|---|---|---|---|---|
| | | H | M | |
| Calc | H | 16 | 1 | 17 |
| | M | 5 | 14 | 19 |
| | | 21 | 15 | 36 |

Zone 1-2

| | | Observed | | |
|---|---|---|---|---|
| | | H | M | |
| Calc | H | 12 | 2 | 14 |
| | M | 1 | 3 | 4 |
| | | 13 | 5 | 18 |

The next two contingency tables explore possible differences due to daytime or nighttime related conditions during the period of tracer release. Releases for tests 3, 4, 5, and 8 are termed nighttime cases; the rest of the tracer releases are during daytime influences (when upward thermal convection is more likely to be significant). The daytime versus nighttime tables show about equal success in relating transport occurrence to tracer sampling.

Daytime (1,2,6,7,9)

| | | Observed | | |
|---|---|---|---|---|
| | | H | M | |
| Calc | H | 14 | 1 | 15 |
| | M | 3 | 12 | 15 |
| | | 17 | 13 | 30 |

Nightime (3,4,5,8)

| | | Observed | | |
|---|---|---|---|---|
| | | H | M | |
| Calc | H | 14 | 2 | 16 |
| | M | 3 | 5 | 8 |
| | | 17 | 7 | 24 |

The next two tables count trajectory "hits" in zones by trajectory type, using either MESONET calculated or tetroon observed trajectories. The tetroon table shows 41 of 54 correct while the MESONET has 39 of 54 correct. These differences between tetroon estimates and calculations using MESONET wind data are probably not statistically significant. However, previous comparisons of tracer transport, tetroons, and MESONET determined trajectories have indicated consistently better estimates by the tetroon flights. Both tables have an apparent bias of underprediction of the total amount (zones) impacted by the $SF_6$ tracer. For each trajectory type, 25 $SF_6$ zone "hits" are calculated and 34 zone "hits" are observed; also, 29 $SF_6$ "misses" are calculated versus 20 observed. A composite of all cases for both tetroon and MESONET determined trajectories are shown in the last table. This result is the same as given for all zones and is presented for comparison with the four preceeding tables.

Tetroons vs SF 6

| | | Observed H | Observed M | |
|---|---|---|---|---|
| Calc | H | 23 | 2 | 25 |
| | M | 11 | 18 | 29 |
| | | 34 | 20 | 54 |

MESONET vs SF 6

| | | Observed H | Observed M | |
|---|---|---|---|---|
| Calc | H | 22 | 3 | 25 |
| | M | 12 | 17 | 29 |
| | | 34 | 20 | 54 |

All Cases

| | | Observed H | Observed M | |
|---|---|---|---|---|
| Calc | H | 28 | 3 | 31 |
| | M | 6 | 17 | 23 |
| | | 34 | 20 | 54 |

About 3/4 of the transport into the six characteristic regions is accounted for by either trajectory method (tetroon observations or calculations using MESONET winds ). There is no large difference in the success of one method compared to the other. Separately, each method identifies about 3/4 of the regional transport correctly; jointly they identify about 5/6 of the regional transport. Each trajectory method is most characteristic of flow at a different altitude in the lower atmosphere. Often the air flows at the two represented altitudes are similar and many of the characteristics indicated by one method are also indicated by the other one. At times, though, the flows may differ substantially from one another. Then, when plume material is inserted into different vertical layers, the observed $SF_6$ impacts are better described by the joint sets of trajectories.

These transport assessments, although somewhat qualitative, are useful indicators. They may be examined in conjunction with the more quantitative comparisons of modeled and observed tracer concentrations presented in Chapter V. The systematic differences which exist in these qualitative comparisons can be expected to propagate into the quantitative comparisons since the model uses these same trajectory calculations. A summarization of these transport assessments is provided in Chapter VI after the discussions from Chapter V have been presented.

## V. Comparisons of concentrations and plume impacts

In the discussion of comparisons which follow, it is useful to incorporate terminology from modern logic or set theory. The concepts of intersections and unions of sets are useful. Assessments of plume effluent transport were examined in the previous chapter. These transport behaviors were categorized using a qualitative concept of empty and non-empty sets for phenomena non-occurrence or occurrence in each of the characteristic zones. A calculated or measured impact either affected a zone or it did not. Thus, these comparisons were qualitative in sense. Four combinations of comparisons between measured and observed concentration impacts were used and depicted in 2x2 contingency tables. Two entries in the contingency table groupings correspond to the set intersections of measured and calculated values (the paired points of jointly null values and the paired points of jointly non-null values). These intersection values correspond to the principal diagonal of the 2x2 table. The other two table entries correspond to groupings in which one of the paired values is null while the other is non-null. These combinations correspond to the union of the sets. In the previous chapter comparisons were made between sets of data groupings which were treated as either empty or non-empty sets. In this chapter some quantitative comparisons of modeled and observed areas of impact and concentrations are considered using actual magnitudes of individual impacts. Agreements and differences between modeled concentrations and amounts of impact will be examined.

A number of possible approaches may be used to develop these comparisons. One of the traditional methods is the plotting of scatter diagrams of calculated versus observed concentrations. Comparisons of individual values may be examined to evaluate the likelyhood that a specific observation will be calculated within a particular level (magnitude) of agreement. The agreement may be dependent upon the magnitude of the observation or other factors. However, the usefulness of (and desired information from) the models and the measurements is not limited to comparisons of specific point "realizations". Typically, the point values (modeled or observed) are generalized to be descriptive of the effects in a specific area or volume, in which there is assumed to be a homogeneous "realization", and these generalized effects are translated into a cumulative effect, total area of impact, etc. Estimates of potential consequences are based on these accumulated or generalized total impacts. These consequences may be derived from either an estimated total impact or from a piecewise accumulation of the several subsets of impacts which comprise the total impact. In any event, the process is essentially the same; it is simply the attempted resolution which differs. Therefore, it is useful to examine the effectiveness of modeling the amount of area impacted by airborne effluent and the effectiveness of modeling the total exposure to airborne effluents. The non-specific terms "dosage" and "impact" will be used interchangably with the term "exposure".

A key concept in the formulation and interpretation of quantitative comparisons is the definition of a "null" value. For measured data the

null value may relate to the minimum detectable concentration or some multiple of the minimum. For the modeled values there is no identical lower limit. At times it would be useful to define a lower limit which is 100 to 1000 times less than the maximum value in the set. In other instances it would be useful to include only those points which most contribute to a certain percentage of accumulated or total impact (for example the set of largest individual values which comprise a summation which is 95 or 99% of the total sum). It is beyond the intended scope of this discussion to treat the topic of limiting bounds of the data values (for example, what is a null value in an absolute sense or in a relative sense). This topic is extremely important to the interpretations and conclusions drawn from the comparisons of calculated and observed data. Likewise, the inclusion of realistic levels of uncertainties in the data and the modeled values is essential to a meaningful interpretation of the comparisons.

The MESODIF model was used to calculate hourly accumulated concentrations of tracer. The modeled tracer experiments were continuous, 8-hour, steady releases of $SF_6$, with atmospheric sampling of 12 to 30 hours duration beginning with the onset of tracer release. The MESODIF computations for each test began at the beginning of tracer release and continued until all of the modeled plume effluent had left the computational area. This duration was typically 18 to 24 hours of modeled time. For the small grid data comparisons, calculated and sampled points are sums of the sets of twelve sequential hourly concentrations. For the large grid, the comparisons are made with individual values of total accumulated impacts.

In the presentations which follow all measurements less than 1% of a maximum reference concentration were defined to be a virtual null. The reference maximum values were identified from the array of summed hourly impacts (for small grid data) or from the particular values (large grid data) during which these virtual null concentrations were defined. (The reference maximum is the maximum of the sum of the 12 hourly values for a small grid test, or the maximum of all samples within a large grid test.) These virtual null values were set to zero for the comparisons only, but not within the archived data set.

Evaluations of both point by point and accumulaterd impacts will be addressed in the following paragraphs. Exposure summations and area coverage impacts will receive the greatest amount of discussion. Some important extensions to the comparisons presented in Chapter IV result when the individual magnitudes or summations of magnitudes are used to describe the amount of tracer impact and the extent of area exposed. The occurrence of joint "hits" or joint "misses" for observed versus calculated comparisons corresponds to groupings which correspond with set intersections. A quantitative description of the intersections of calculated and observed data will be provided. Three basic features of plume impact are examined. They are 1) total area coverages of the paired sets of calculated and observed concentration data, 2) total exposures, and 3) the set intersections for 1) and 2). A brief commentary on these agreements and disagreements concludes the chapter. Summarization of these comparisons follows in chapter VI.

Comparisons of modeled versus observed large grid impacts are made first for tests 6, 7, 8, and 9, including area or coverage of impact, total concentration impact, and the intersections and unions of the corresponding sets. The analogous comparisons for all nine small grid tests follow. Large grid $SF_6$ concentration measurements for tests 1-5 are believed to be of qualitative use and were utilized in chapter IV. However, because these data have limited completeness and accuracy, they are not used for the quantitative comparisons which follow. The large grid evaluations based upon tests 6-9 are believed to be representative of the full set of test data from the large sampling grid. Since the test 6 data contain more uncertainty than the test 7, 8, or 9 data , test 6 indications should be considered somewhat less reliable. Discussions of sample quality have been provided in the data volume (Start, et al, 1984, Appendix H).

The initial and most simple quantitative examination of calculated versus observed concentrations is provided by scatter diagram plottings of paired values. Figure V-1 illustrates paired data for test 8 in which the large grid sampling values are related to the total accumulated impact calculated using the MESODIF model. The null and virtual null values are plotted along the top and right-hand axes of Figure V-1. For this particular test, an examination of the figure reveals the following features. There were no non-null values calculated for locations at which a null value was observed (points along the right-hand axis). Many null values were calculated for locations which did not have a null (points along the top axis). These null and virtual null values along the axes correspond to the union of the sets of calculated and observed concentrations. The points within the interior of the figure and the point on the axes at the upper right-hand corner correspond to the intersection of the sets. These are the points which agree with each other in the sense of being jointly null or jointly non-null. The magnitudes of individual paired values are within a factor of 10 of being in quantitative agreement with their paired counterpart. There appears to be systematic undercalculation of impacts by about a factor of two or three. This behavior will be addressed in more detail in later paragraphs.

Scatter diagrams of point by point types of comparisons for the other IFX tests are provided in Appendix A. Those diagrams also display a large amount of difference between calculated and observed values, as expected. Plots for individual hourly values typically exhibit even more scattering. There are many possible reasons for these scatterings. One reason is the general lack of homogeneity of the transporting and diffusing conditions; spatial inhomogeneities usually exist within the IFX study region. Plume transport and diffusion processes also can be influenced significantly by random stochastic events which occur infrequently at any one location during the period of measurements. When this happens, the observed plume behavior will seem erratic and highly variable from test to test and within subintervals of a test. That is, if sub-grid scale and sub-time scale phenomena predominate the behavior of the atmosphere during the measurement period, the observations will usually be irregular and poorly predicted by models on a point-by-point basis.

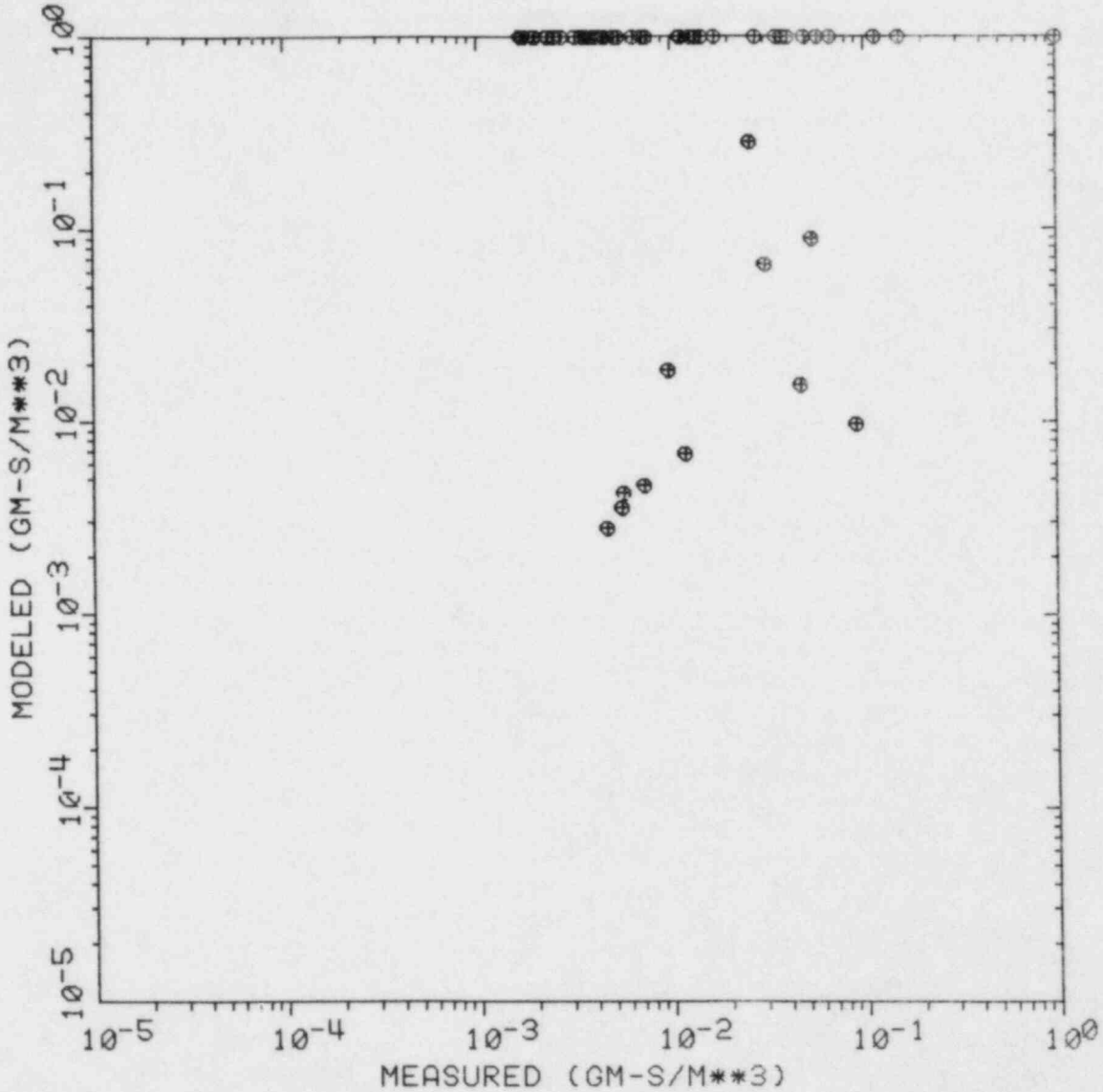


Fig. V-1 Comparison of measured versus modeled plume exposures (gm-sec/m3) for test 8, large-grid data.

Comparisons of area coverage of concentration patterns (transport phenomena to a large extent) and total impact (analogous to the sum of concentrations) are made for modeled versus observed values. In order to prepare the data for these types of comparisons it is necessary to specify either an area weighting technique for the concentration observations (which are not always evenly spaced throughout the grid) or to specify a spatial interpolation technique to place the observed concentrations onto a uniform computational array. A spatial interpolation technique is utilized. The details of the interpolation technique are presented in Appendix B.

The preparation of the tracer sampling observations for these comparisons included the following treatments. For the large grid $SF_6$ concentration data were entered, and interpolated when necessary, onto a grid with 6 km spacing (the same as the samplers). For the small grid $SF_6$ concentrations were entered and interpolated onto a grid with 1 km spacing. This spacing was the same as sampler spacing near the source; at the greater distances sampler spacing was 4 km and more interpolation was necessary. For both groups of data a test by test lower limit for significant $SF_6$ concentration was set. This value was 0.01 times the maximum observed concentration. This limit typically had little effect on data in the large grid. For the small grid assessments, the grid point concentrations were sums of the 12 sequential hourly samples. These sums were formed before the maximum was determined and the lower limit was set. The likelihood of deleting significant data from the small grid sets was substantially reduced because the summing process tended to smooth and reduce the gradients of concentration impact. (Additional discussion of computational methods are contained in Appendix B.)

Composite patterns of tetroon and MESODIF calculated trajectories are included in chapter IV. The corresponding isopleths of 30-hour $SF_6$ tracer concentrations (units are parts per trillion) for tests 6 through 9 are shown in Figures V-2 through V-5. Test 6 isopleths in Figure V-2 show a relatively simple pattern of concentrations which were strongly influenced by down-valley winds following frontal passage. The test 7 isopleth pattern in Figure V-3 is the result of up-valley winds. Eventually, these winds weakened and turned counterclockwise so that up-canyon flow into zone 6 developed. Later, weak down-canyon and down-valley flow occurred until the return of strong up-valley winds with solar heating after sunrise. Test 8 isopleths, shown in Figure V-4, developed during persistent, nocturnal down valley winds. Up-valley winds resumed during late morning and transported plume material rapidly up-valley. Isopleths for test 9 are shown in Figure V-5. Test 9 plume transport and diffusion occurred initially during coasting up-valley winds. Late at night the up-valley winds slowed and reversed so that some plume material moved southwestward back across the study area. Late the next morning up-valley winds recurred and transported material out of the study area.

The number of computation grid area units (number of boxes) with $SF_6$ concentrations above the lower threshold were counted for both observed and calculated tracer impacts. Sums were formed from

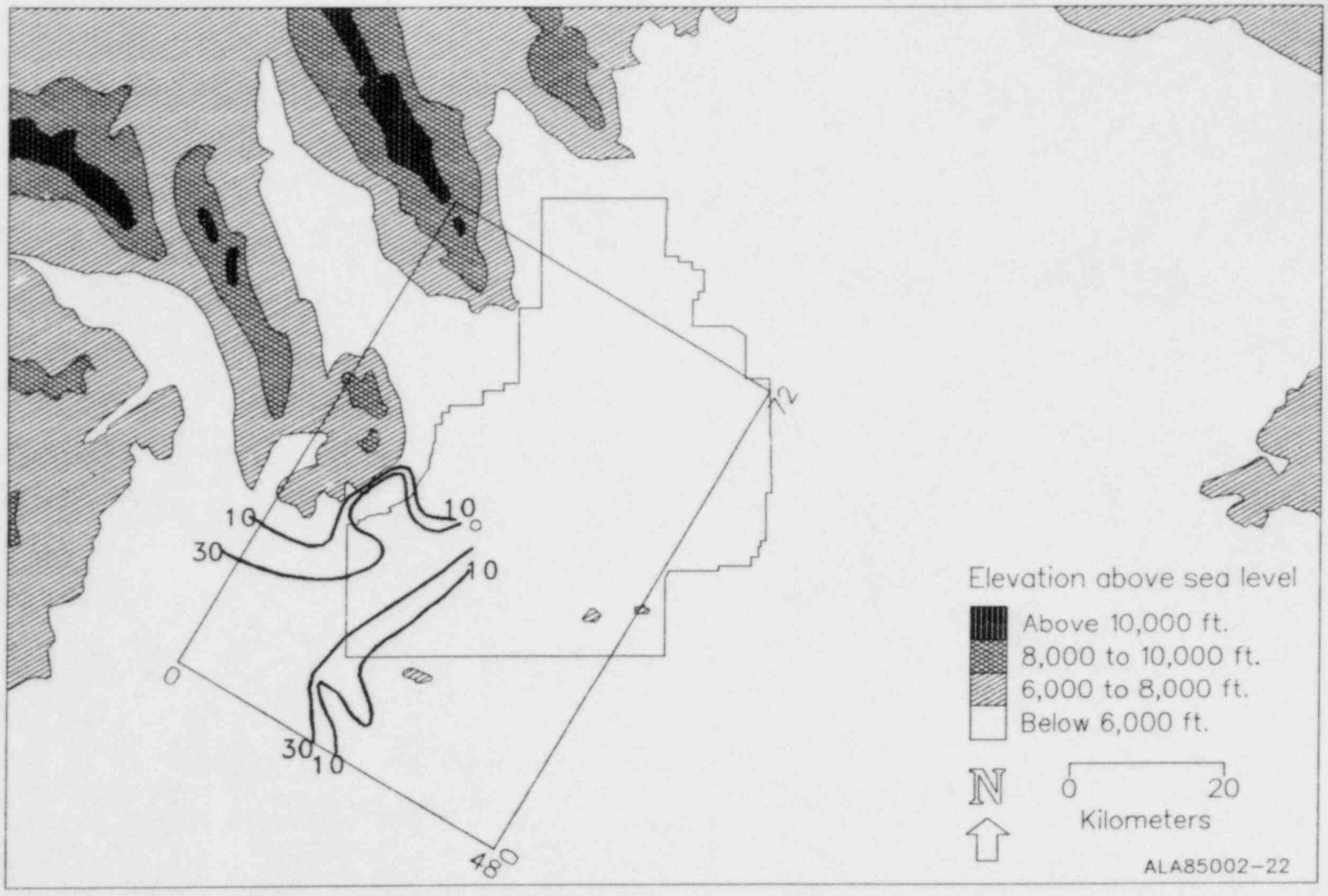


Figure V-2. Large grid tracer isopleths, test 6

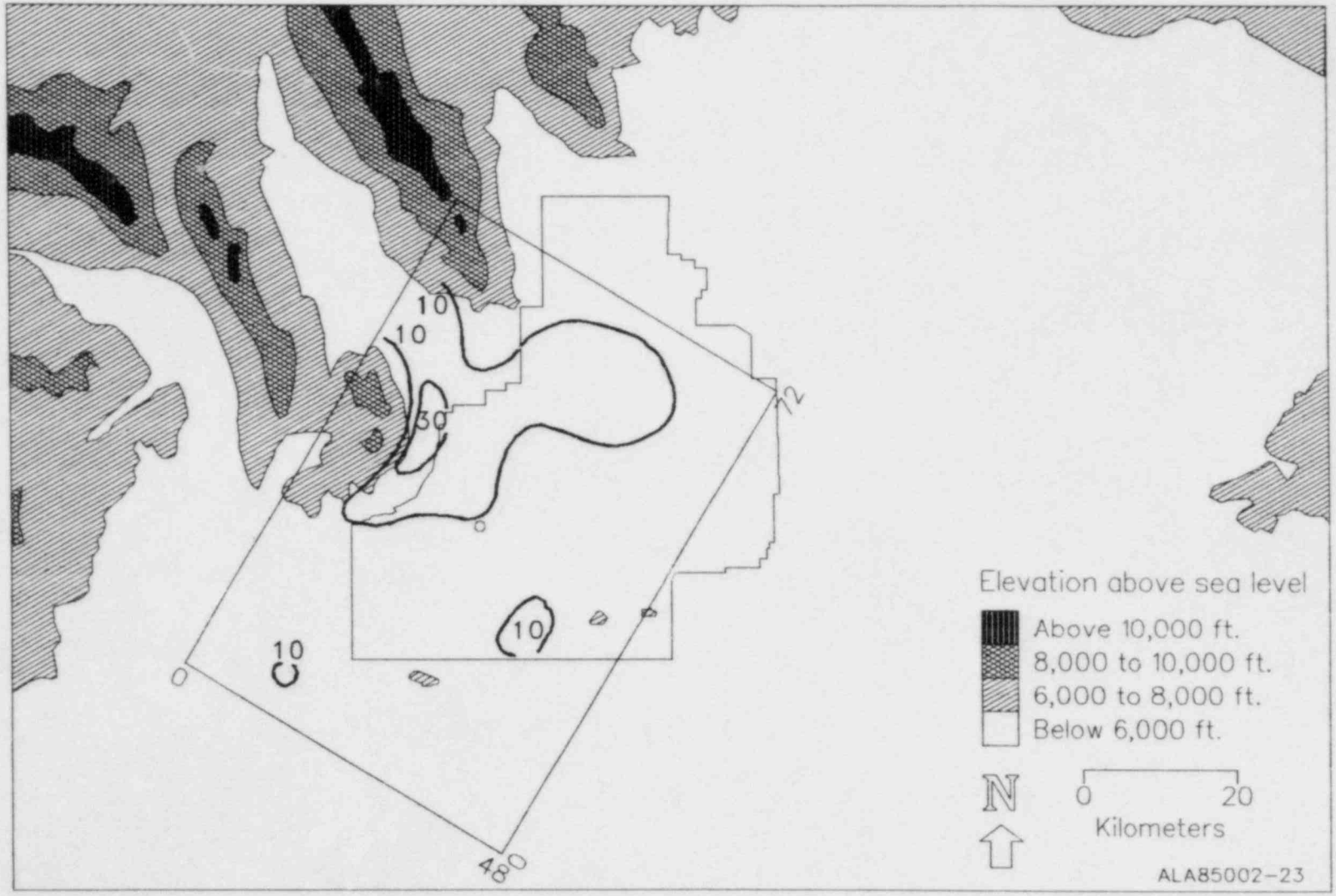


Figure V-3. Large grid tracer isopleths, test 7

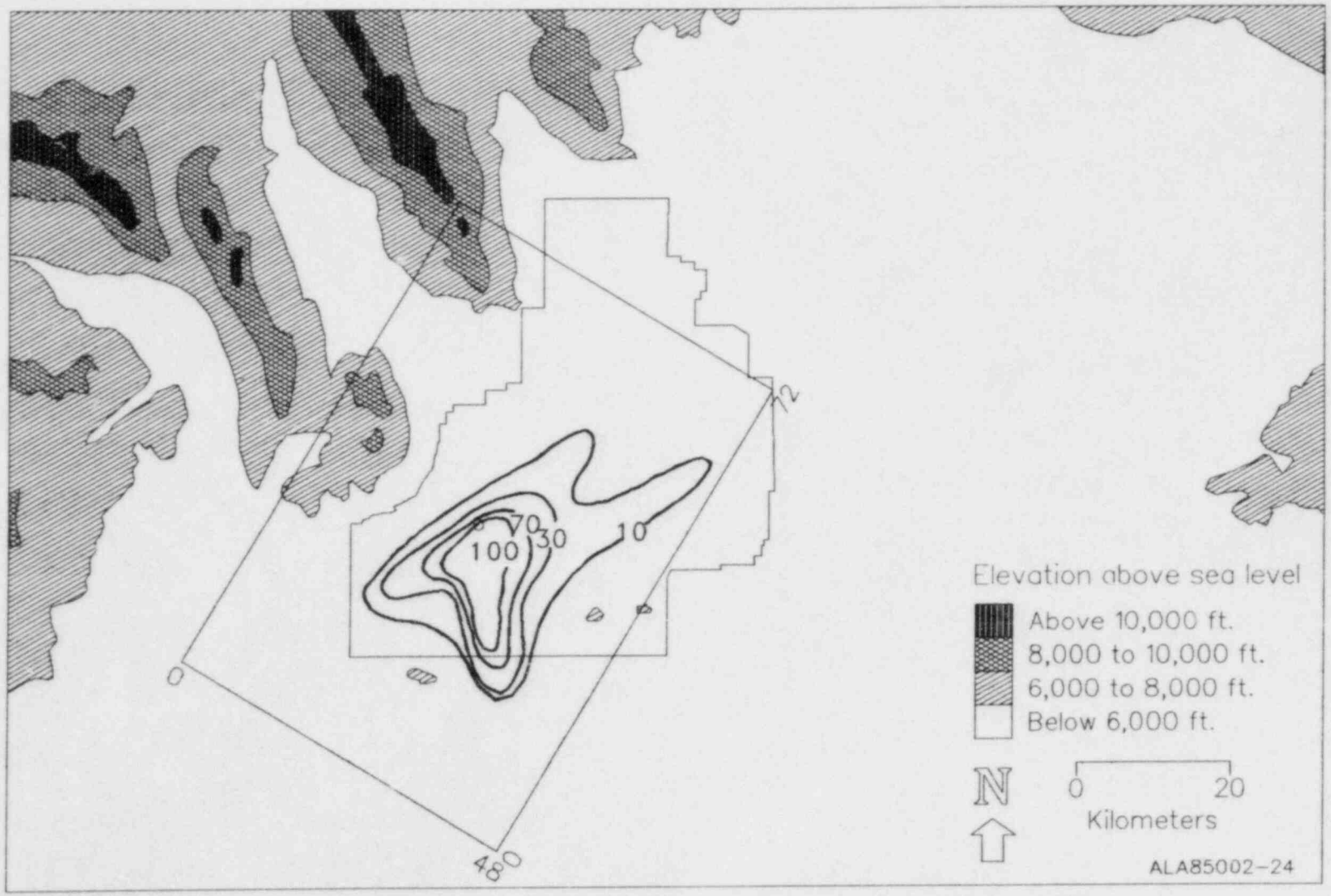


Figure V-4. Large grid tracer isopleths, test 8

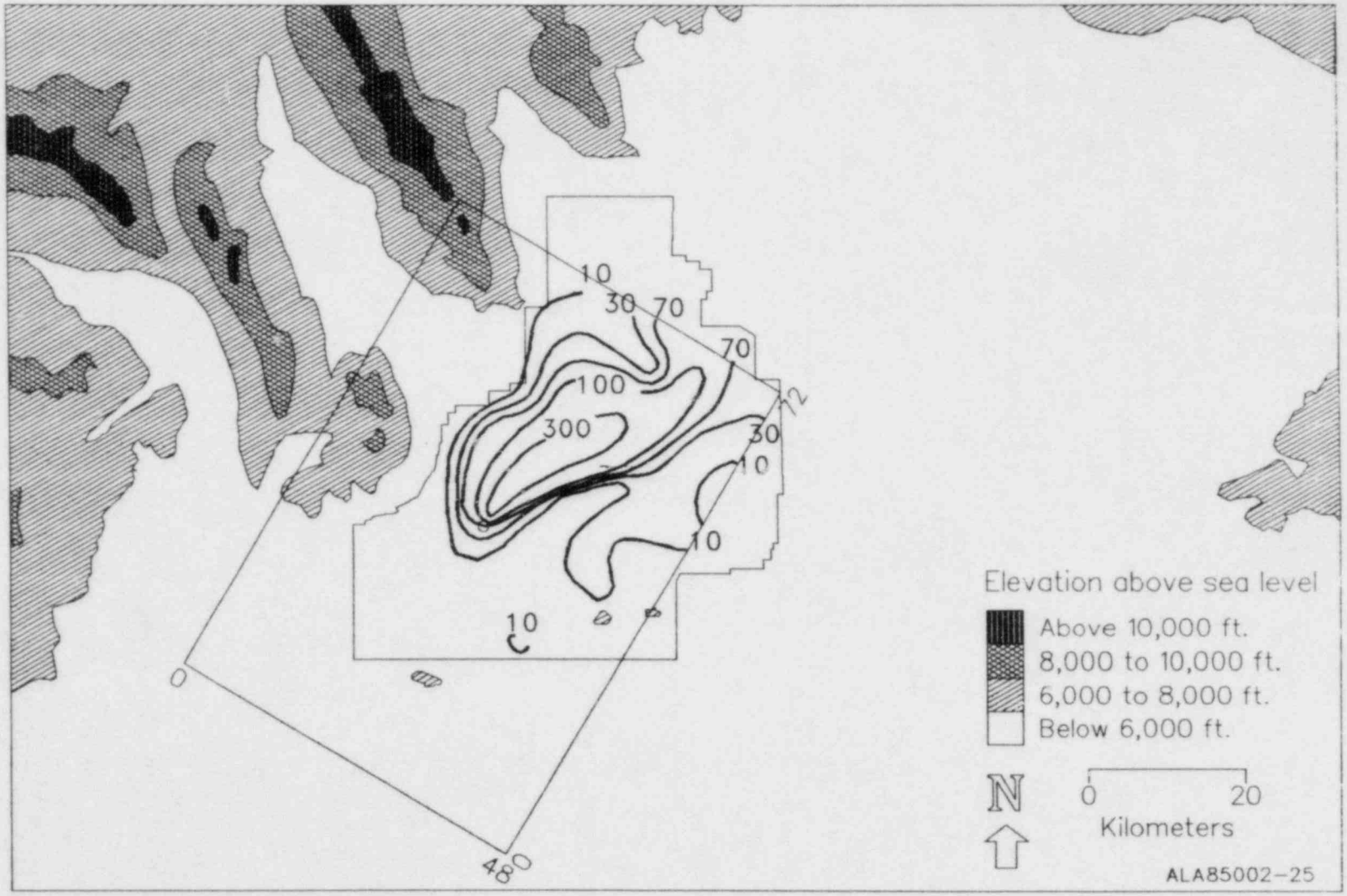


Figure V-5. Large grid tracer isopleths, test 9

concentration values greater than the virtual null values. These results are listed in Table V-1.

The information in Table V-1 suggests the following conclusions. Calculated total areas are less than half (42%) of the observed total areas of plume impact. Over 3/4 of the model determined impact areas (81%) are coincident with their counterpart observed areas. About 2/3 of the observed total concentration impacts (66%) are calculated by the MESODIF model; there were substantial differences from test to test. Over 3/4 of the calculated concentration impacts (86%) are coincident in location with their counterpart calculated impacts. In general, the model calculations specify impacts in the correct locations (81%) but the spatial extents of impact are systematically underestimated (42%). Calculated concentration impacts (sums of concentration weighted areas) are about 2/3 of their counterpart observed impacts.

Table V-1. Results of comparisons for large grid data and calculations.

| Total Area Number of Blocks (36 $km^2$/block) | | | | Concentration Impact Sum of Concentrations x Area | | | |
|---|---|---|---|---|---|---|---|
| Test | Calc | Obs | Intersection | Test | Calc | Obs | Intersection |
| 6 | 27 (55%) | 49 | 23(85%) | 6 | .35(33%) | 1.07 | .30(85%) |
| 7 | 43 (48%) | 90 | 29(67%) | 7 | .76(200%) | .38 | .50(66%) |
| 8 | 11 (19%) | 59 | 11(100%) | 8 | .50(46%) | 1.09 | .50(100%) |
| 9 | 19 (45%) | 42 | 18(95%) | 9 | 1.13(69%) | 1.63 | 1.07(95%) |
| Sum | 100 (42%) | 240 | 81(81%) (of 100) | Sum | 2.74(66%) | 4.17 | 2.37(86%) (of 2.74) |

Obs: denotes the number of observed area blocks (or sum of concentration weighted area blocks) with $SF_6$ concentrations above the threshold levels.

Calc: represents the calculated values and its percentage of the observed data.

Intersection: describes the amount of calculated effects which are coincident in location with observed effects.

Patterns of concentration isopleths may be developed from the small grid tracer concentration data, but are not presented in this report since the analyses would serve no special purpose for the quantitative comparisons which follow. Additional impact comparisons, which correspond to the large grid treatments, are made for all tests using the data from the small grid. These results are listed in Table V-2.

The results for the small grid comparisons are very similar to the large grid comparisons, with the following exceptions. The percentages of coincident total areas average larger for the small grid. In general, if the MESODIF model calcuated an impact area, it is almost a certainty that it is part of the observed total area of impact. Most of the set of model calculated areas intersect the set of areas of sample impact. The calculated area coverage in all cases is less than the area coverage of the observed data fields. The model generally transported the plume to the correct areas of the grid but did not spread the material enough or retain it over the receptor points long enough to provide coverages and total impacts fully comparable to the observations.

Table V-2. Results of comparisons for small grid data and calculations.

| | Total Area Number of Blocks (1 $km^2$/block) | | | Concentration Impact Sum of Concentrations x Area | | |
|---|---|---|---|---|---|---|
| Test | Calc | Obs | Intersection | Calc | Obs | Intersection |
| 1 | 103 (31%) | 335 | 99(96%) | 1.60 (55%) | 2.92 | 1.59(99%) |
| 2 | 106 (19%) | 547 | 99(93%) | 1.14 ( 9%) | 13.2 | 1.09(95%) |
| 3 | 389 (63%) | 617 | 388(100%) | 18.3(152%) | 12.0 | 18.2(100%) |
| 4 | 248 (47%) | 527 | 227(92%) | 4.62 (74%) | 6.26 | 3.71(80%) |
| 5 | 145 (24%) | 615 | 141(97%) | 18.7 (95%) | 19.6 | 18.2(97%) |
| 6 | 135 (79%) | 170 | 120(89%) | 6.79 (53%) | 12.8 | 4.92(73%) |
| 7 | 144 (42%) | 340 | 143(99%) | 5.00(109%) | 4.56 | 4.84(97%) |
| 8 | 192 (43%) | 444 | 179(93%) | 14.8 (61%) | 24.4 | 14.3(96%) |
| 9 | 96 (47%) | 204 | 95(99%) | 2.91 (26%) | 11.3 | 2.90(100%) |
| Sums | 1558 (41%) | 3799 | 1491(96%) | 73.9 (69%) | 107. | 69.8(94%) |

VI. Discussion and summary of comparisons.

The nine cases of intensive meteorological and gaseous tracer measurements have been described in general terms. The tracer data from these tests, along with tetroon trajectories and a limited subset of meteorological observations, were used to formulate qualitative indications (Chapter IV ) and quantitative comparisons (Chapter V ) of the consistency of observations with calculations. The results of these comparisons are summarized in the following paragraphs. Some possible reasons for differences and agreements are noted.

The findings of Chapter IV suggest that transport into the six characteristic zones of tracer impact are correctly identified about 75% of the time by using either MESODIF calculated trajectories or tetroon marked trajectories. If both trajectory types are pooled together, the percentage of correctly identified zones increases to 83%.

The findings of Chapter V, based on MESODIF modeled trajectories, show that about 40% of the area impacted by $SF_6$ gaseous tracer is calculated to be impacted by MESODIF modeled tracer behaviors. The intersections of modeled and observed arrays of impact areas are significant. For the small grid, 94% of the calculated areas correspond to observed impact areas. For the large grid this percentage is about 80%. The concentration impact comparisons closely parallel the findings for transport and trajectories. Calculated total impacts account for about 2/3 of the observed total impacts. Large and small grid impacts are 66 and 69% of the observed amounts when each type is pooled for all tests. The difference in these average percentages is probably not statistically significant. (The intersections of the arrays of calculated and observed impacts result in large correspondence of modeled to observed behaviors.) For the large grid 86% of the calculated impacts are coincident with observed impacts; for the small grid 94% are coincident.

The timing (the WHEN consideration) for impact occurrences has not been investigated. The basic questions of where impacts occurred and how much impact occurred have been addressed. In both instances the calculated area coverages and the total impacts are biased toward being too small compared to observations.

Some possible reasons for this bias toward under-calculation are the assumption of a Gaussian distribution in the horizontal and the poor characterization of vertical exchange phenomena. Earlier investigations (e.g. Sagendorf and Dickson (1974); Start, et al., (1971)) have shown that some calculations based upon a Gaussian plume spread parameter, sigma-y (e.g. Turner, 1970; Yanskey, et al., 1966), have substantially underestimated observed horizontal plume widths. Vertical exchange phenomena, especially during times of stable stratification of the atmosphere, are important. The vertical characteristics of IFX plumes are probably not modeled well using the customary values of sigma-z and the assumption of a Gaussian vertical mass distribution. Tracer release personnel and other study participants reported nightime visual observations of IFX oil fog plumes in which aperiodic, stochastic

turbulent events transported plume segments to near ground level. Blackadar (1957) and others have discussed these periodic nighttime turbulent bursts or episodes which occur in the nocturnal boundary layer. When portions of the tracer plumes are captured by these bursts and carried downward to near the surface, some of the plume mass is believed to remain in the completely different, low-altitude transport and diffusion environment. It probably remains there with little chance of upward transport to the atmospheric height at which it originated until daytime convective mixing destroys the shallow surface layer in which it is contained. The result of such vertical displacement may be low-altitude, stagnant pockets of higher $SF_6$ concentration, transport to a substantially different location of impact, or both.

A wind direction variation may develop in characteristic zone 5, near the mountains to the northwest of Grid III. Systematic wind field distortions and recirculations seem to occur in that locale and are not directly observed by the MESONET system. No MESONET wind station is located in the area to observe the phenomenon. Visual observations of low-altitude clouds by meteorologists during other years and radar tracked tetroon trajectories from other studies have suggested this behavior occurs in zone 5. Small scale topographic features such as lava flows, small knolls, or shallow depressions are also responsible for localized transport distortions in the stable layer next to the surface. The findings of Sagendorf and Dickson (1974) have shown that low-altitude pockets of tracer produce significant variations in ground-level sampled tracer distributions.

An important component of simulations is the proper understanding and usage of model calculations and comparisons with measurements. The many communities of experimentalists, modelers, and information users are sometimes at odds because this issue is not well addressed. All model calculations and data sets have associated levels of uncertainty and the atmosphere is characterized by lacks of homogeneity and stationarity. As a result, there are basic limitations to what may be adequately represented by models and a finite set of observations. These limitations do not mean that the observations or modeling results are of little value. Individual values may be correct but of limited suitability for a specific usage. Sub-grid scale phenomena and a lack of homogeneity must be considered as important sources of uncertainty in the resolution of the observations and as contributors to the inability of models to describe small details of atmospheric transport and diffusion. A limited or selected usage of a data set or model may be quite useful in certain situations but the propagated limitations due to the assumptions or treatments should be carefully noted. The definition of a "null" value is another consideration during the formulation and interpretation of quantitative comparisons. These nulls are the limiting minimum values of variables relative the their thresholds of measurement or to their relevance for effects under consideration. Statements of realistic levels of uncertainties for the data and the modeled values are essential to a meaningful interpretation of the comparisons and to a proper application of results from modeling calculations.

## VII. Recommendations

A number of additional studies are appropriate for the IFX data set. Additional diagnostic exercises could be performed to explore the details of the meteorological conditions during IFX cases. Upper air winds and temperature soundings have not been examined in detail, nor have the spatial and temporal changes of winds been studied. Characteristic space and time scales should be determined for the IFX study region. The temporal behavior of tetroons and tracer plumes within the small grid could be examined and compared to meteorological data and modeling results. Other evaluations of the $SF_6$ tracer concentration data could be made such as an examination of differences of modeled and measured paired values versus distance of plume travel.

The MESODIF model should be reviewed for possible modification following these comparisons with IFX data. While MESODIF had success in describing plume transport and diffusion, there seems to be systematic bias toward under calculation of both area of coverage and sums of concentrations. Model calculation sensitivities to inclusion of vertical shear of wind direction and alternate plume mass distributions should be investigated.

Additional comprehensive measurements in the IFX setting could explore those phenomena which may be the sources of much of the differences between calculations and observations. Studies of the behavior of canyon wind flows and their coupling to meteorology over the IFX study domain could extend the understanding of local area transport and diffusion phenomena. Detailed investigations are needed for nocturnal turbulent episodes, vertical diffusion during stable stratifications, the effects of vertical shear of wind direction, as well as the joint effects of these behaviors during nocturnal conditions.

Two important tasks of the modeler are the parameterization of those phenomena which are not suitably resolved by either the data or the model and the estimation of the uncertainties which result from the necessary parameterizations. Without the estimates of uncertainties, an important basis is lacking for judging the significance of differences between observations and model performances. This treatment is extremely important to the interpretations and conclusions drawn from the comparisons of calculated and observed data and to the usage of modeling information. The estimation of limiting uncertainties should be investigated and suitable techniques identified. The application of those techniques could provide a helpful basis for the prioritization of research efforts between model developments, measurement programs, and technique assessments, as well as reduce the likelyhood of unchallenged, non-scientific assertions about the quality and applicability of specific measurements and modeling calculations.

## References


Abbey, R. F. Jr., (1982): Atmospheric Dispersion Research Program, Third Joint Conference on Applications of Air Pollution Meteorology, Jan. 11-15, 1982, San Antonio, Tex. Published by the Am. Met. Soc., Boston, Mass.

Blackadar, A. K., (1957): Boundary Layer Wind Maxima and their Significance for the Growth of Nocturnal Inversions, Bull. of the Am. Met Soc., Vol. 38, No. 5, May, 1957, pp 283-290.

Sagendorf, J. F. and C. R. Dickson, (1974): Diffusion Under Low Wind Speed, Inversion Conditions. NOAA Tech Memo., ERL ARL-52, Air Resources Laboratories, Idaho Falls, Idaho.

Start, G. E. and L. L. Wendell, 1974: Regional Effluent Dispersion Calculations Considering Spatial and Temporal Meteorological Variations. NOAA Tech. Memo., ERL ARL-44, Air Resources Laboratories, Idaho Falls, Idaho.

Start, G. E., C. R. Dickson, and P. G. Voilleque' "Comparisons among Tracer, Tetroon, and Wind-field Derived Trajectories and Some Diffusion Estimates," published in the Proceedings of the Symposium on Air Pollution, Turbulence and Diffusion, December 7-10, 1971, at New Mexico State University.

Start, G. E., J. H. Cate, C. R. Dickson, J. F. Sagendorf, and G. R. Ackermann, 1983: 1981 Idaho Field Experiment, Volume 1, Experimental Design and Measurement Systems, NUREG/CR-3488, Vol.1., Air Resources Laboratories, Idaho Falls, Idaho.

Start, G. E., J. F. Sagendorf, G. R. Ackermann, J. H. Cate, N. F. Hukari, and C. R. Dickson, 1984: 1981 Idaho Field Experiment, Volume 2, Measurement Data, NUREG/CR-3488, Vol.2., Air Resources Laboratories, Idaho Falls, Idaho.

Turner, D. B. (1970): Workbook of Atmospheric Dispersion Estimates, Public Health Service Publication No. 999-AP-26, PB-191482. U. S. Department of Health, Education, and Welfare, Public Health Service, Div. of Air Pollution, Cincinnati, Ohio, 88 pp.

U. S. Nuclear Regulatory Commission. Regulatory Guide 1.111. Methods for Estimating Atmospheric Transport and Dispersion of Gaseous Effluents in Routine Releases from Light-Water Cooled Reactors. USNRC Office of Standards Development, Washington, D. C.

Wendell, L. L., (1972): Mesoscale Windfields and Transport Estimates Determined from a Network of Wind Towers, Monthly Weather Rev., Vol. 100 (7), pp 565-578.

Yanskey, G. R., E. H. Markee, Jr., A. P. Richter (1966): Climatography of the National Reactor Testing Station, IDO-12048, U. S. Atomic Energy Commission, Idaho Falls, Idaho, 184 pp.

# APPENDIX A
## Plots of calculated versus observed $SF_6$ concentrations

Scatter diagrams of point by point types of concentration comparisons for IFX tests are provided. The units of these calculated and observed concentrations are gram-seconds per cubic meter ($gm\text{-}s/m^3$). Accuracies and uncertainties for the $SF_6$ tracer concentrations are given in the introduction of Volume 2, Start et al, (1984). The threshold concentration level adopted is 2.5ppt (v/v) or $1.6 \times 10^{-8}$ $gm/m^3$, which was a typical signal noise level in the ECGC analysers. Above 25ppt (v/v) the absolute $SF_6$ concentrations are expected to be within $\pm$ 10% of their stated values. The largest small-grid, one-hour concentration is less than 2000ppt; the maximum large-grid concentration value is less than 500ppt.

For the small grid data comparisons, calculated and sampled points are sums of the sets of twelve sequential hourly concentrations. For the large grid, the comparisons are made with single values of total accumulated impacts. The diagrams display a large amount of difference between calculated and observed values, as might be expected. Plots for individual hourly values from the small grid typically exhibit even more scattering.

In the presentations which follow all measurements less than 1% of a maximum reference concentration were defined to be a virtual null . The reference maximum values were identified from the array of summed hourly impacts (for small grid data) or from the particular values (large grid data) during which these virtual null concentrations were defined. (The reference maximum is the maximum of the sum of the 12 hourly values for a small grid test, or the maximum of all samples within a large grid test.) These virtual null values were set to zero for the comparisons only, but not within the archived data set. The usefulness of this type of comparison (the limited lower range of values) arises because the calculated and modeled concentrations have a large range of values. The attention is focused upon the largest valued points which contribute most to the quantitative impact. Those points which contribute least to the estimated total impacts are set aside during these visual examinations.

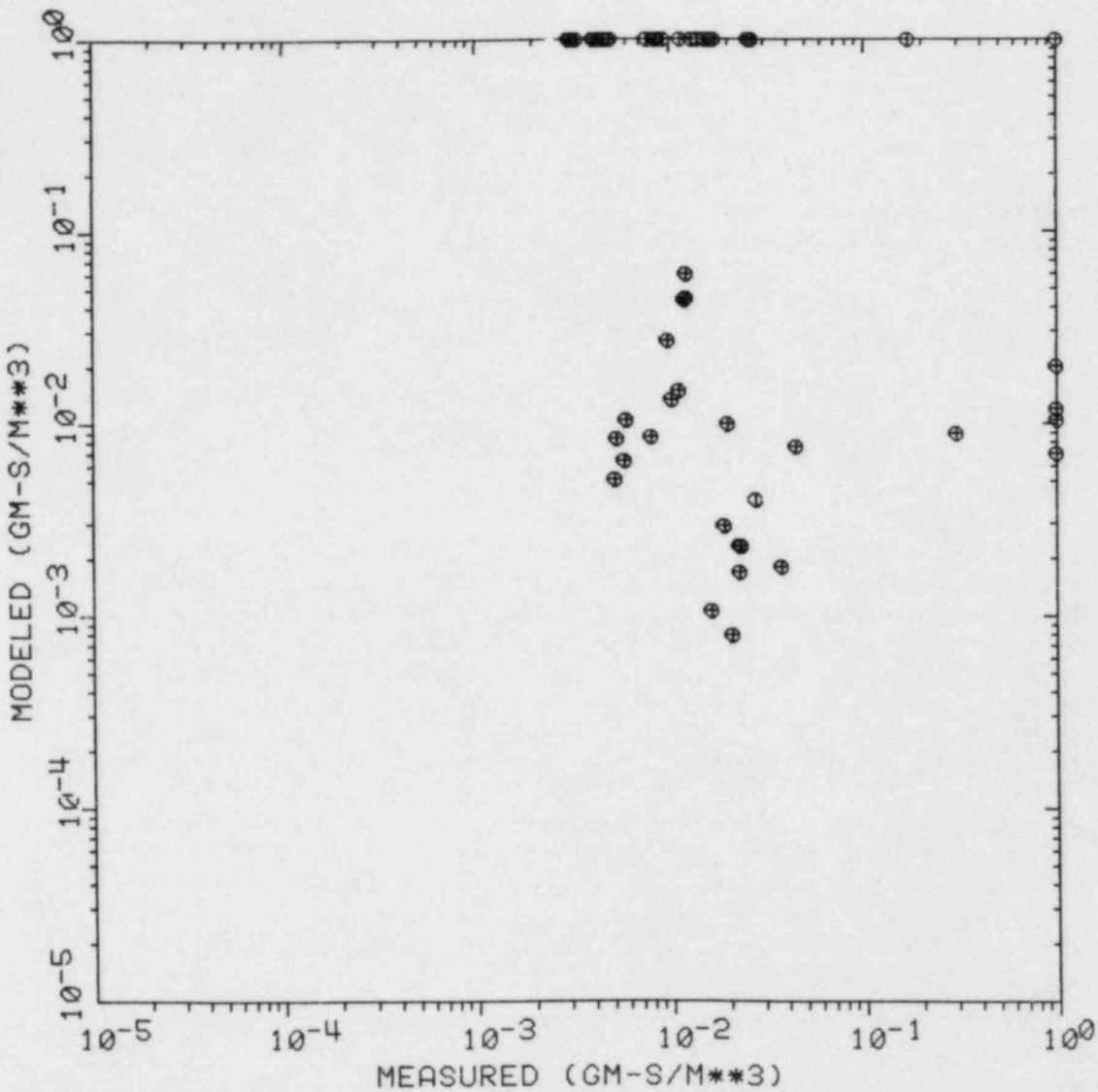


Fig. A-1 Calculated versus observed concentrations for large grid, test 6

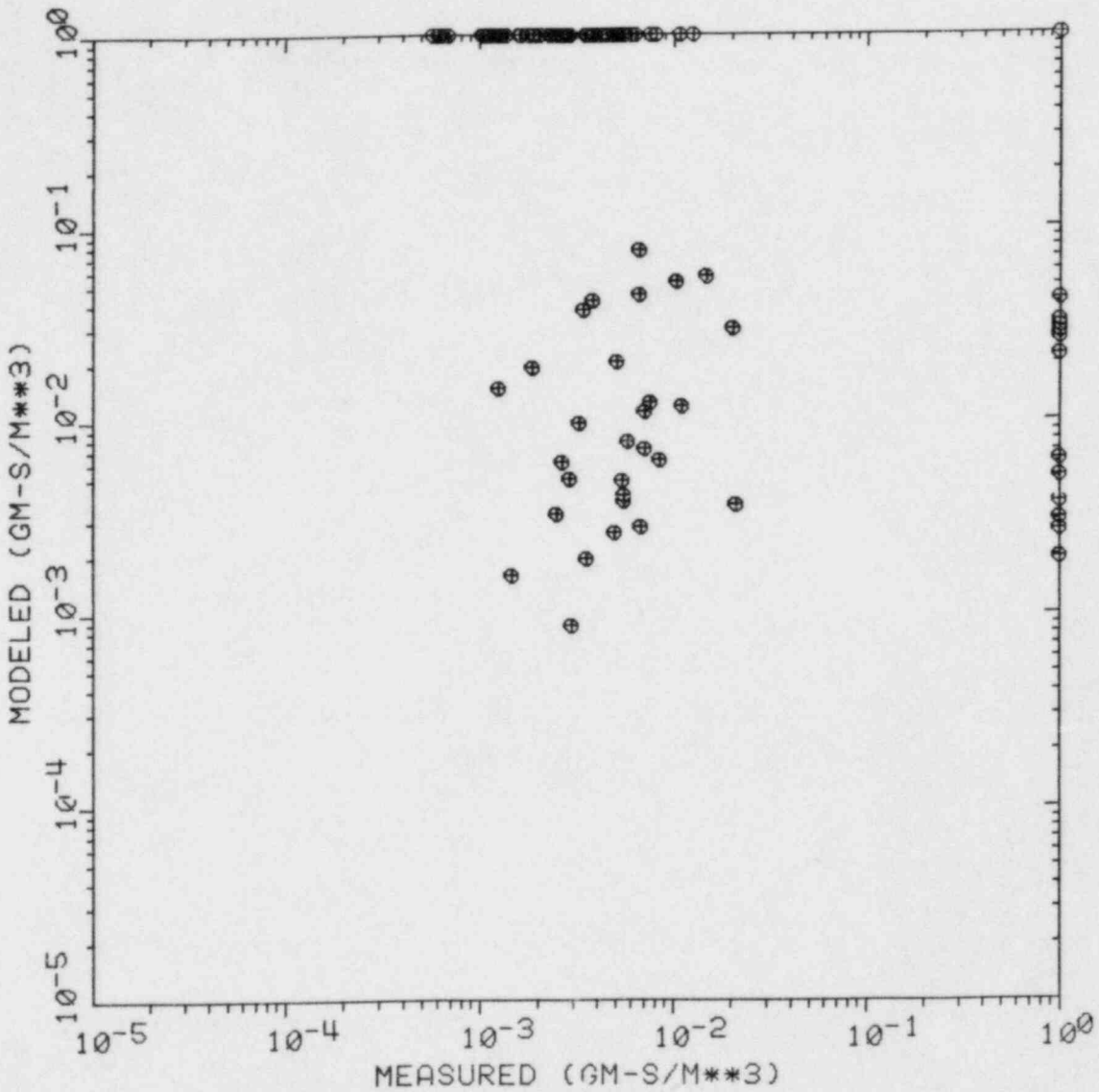


Fig. A-2 Calculated versus observed concentrations for large grid, test 7

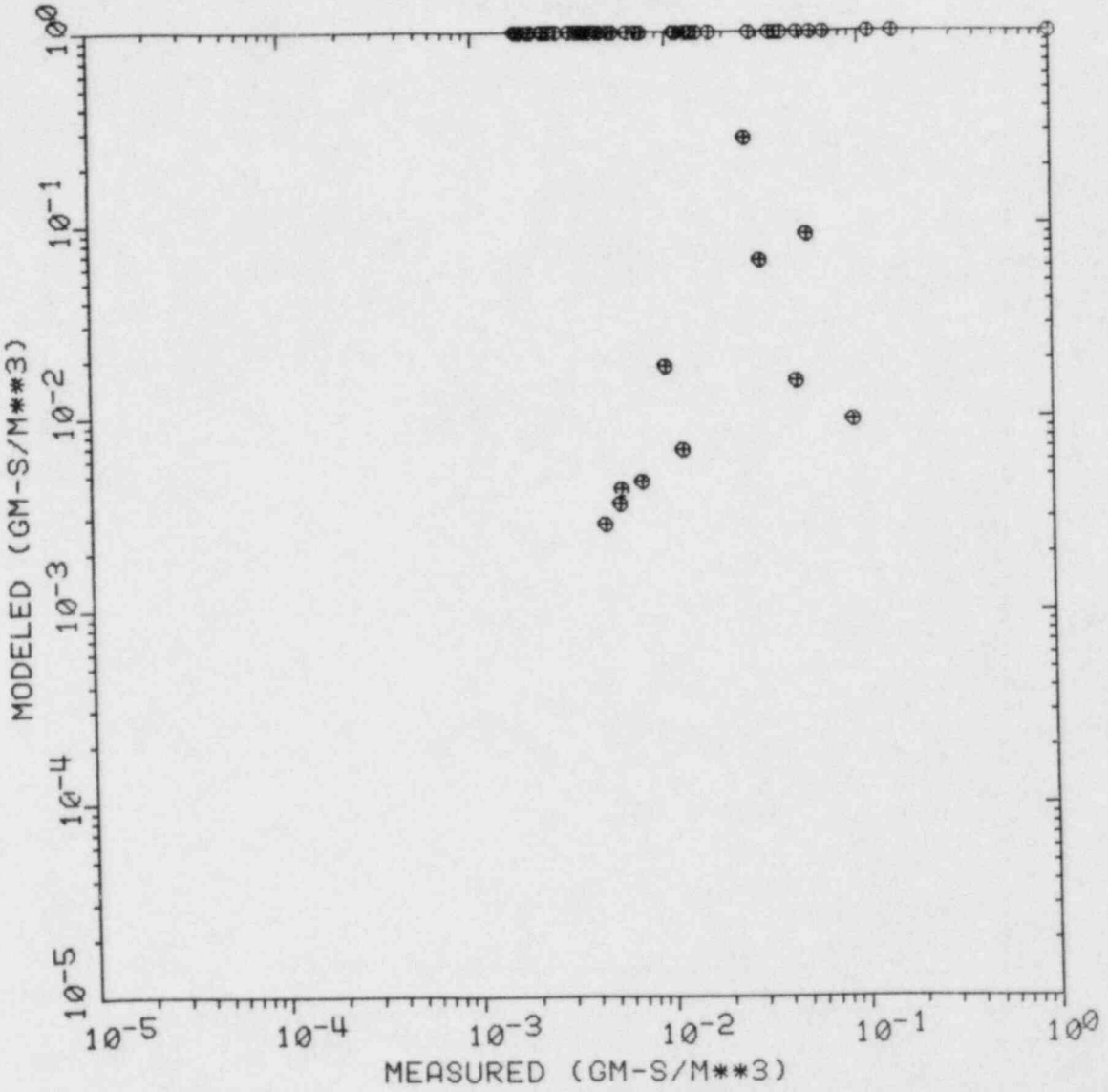


Fig. A-3 Calculated versus observed concentrations for large grid, test 8

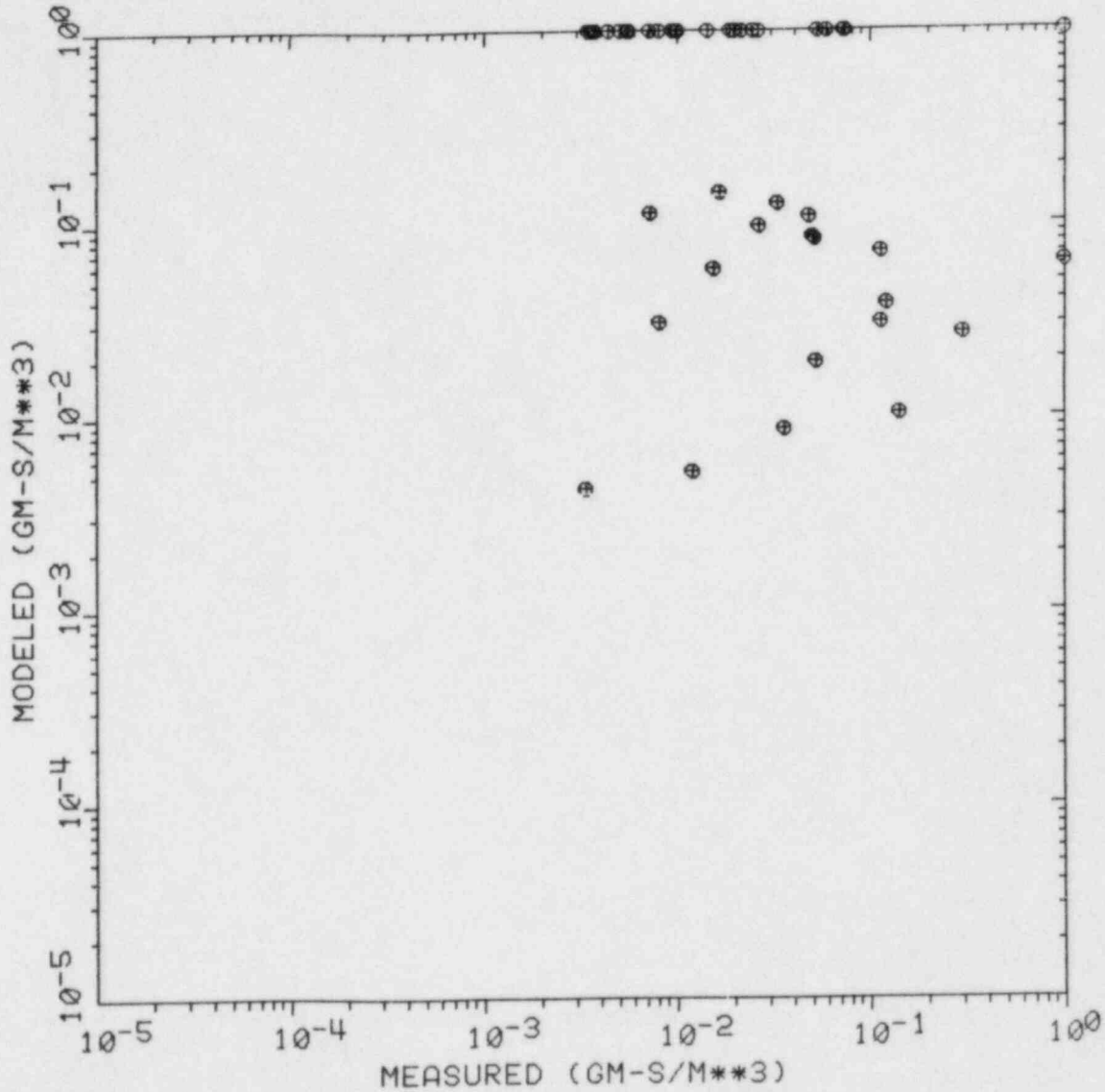


Fig. A-4 Calculated versus observed concentrations for large grid, test 9

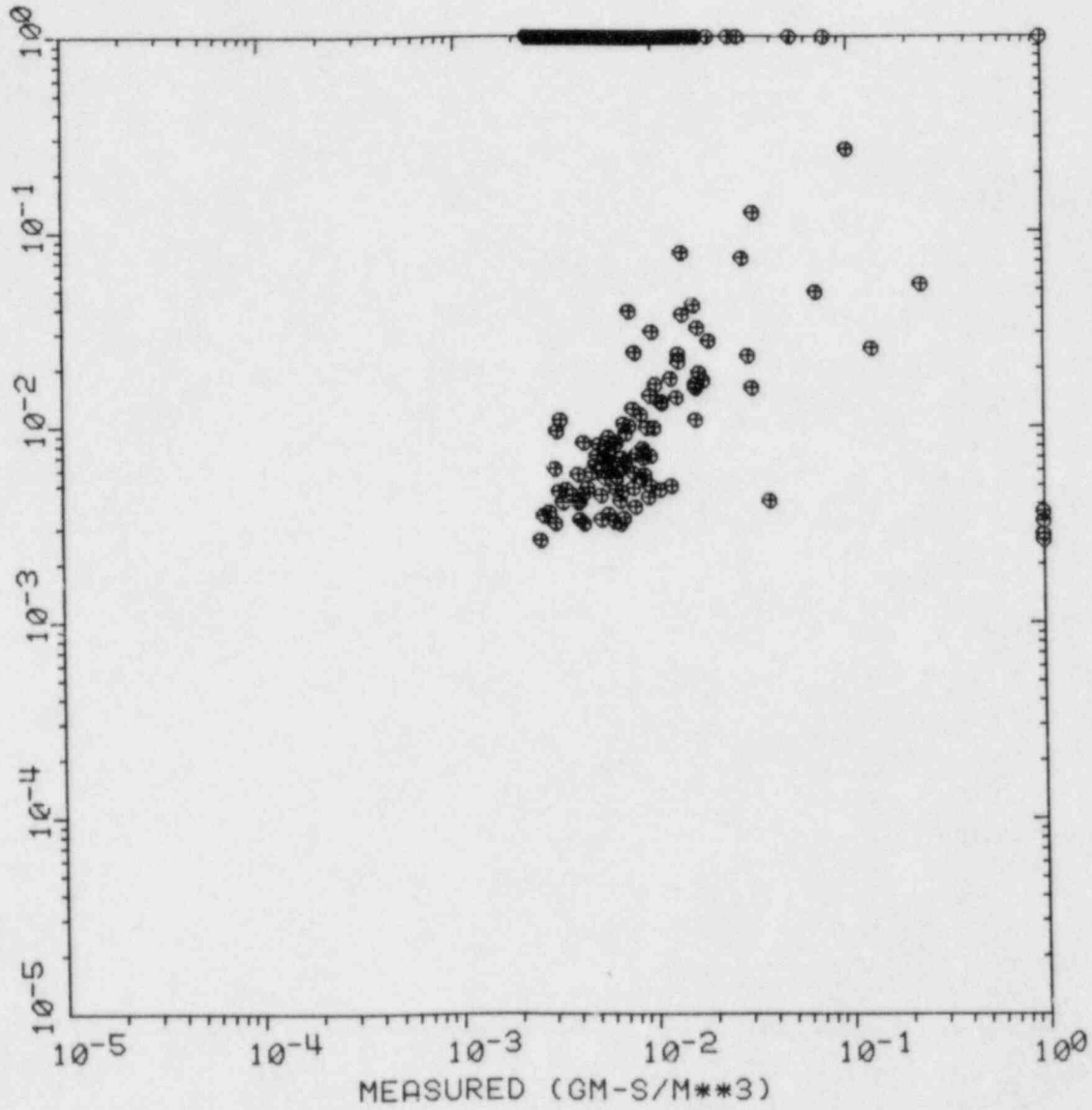


Fig. A-5 Modeled versus observed concentrations for small grid, test 1

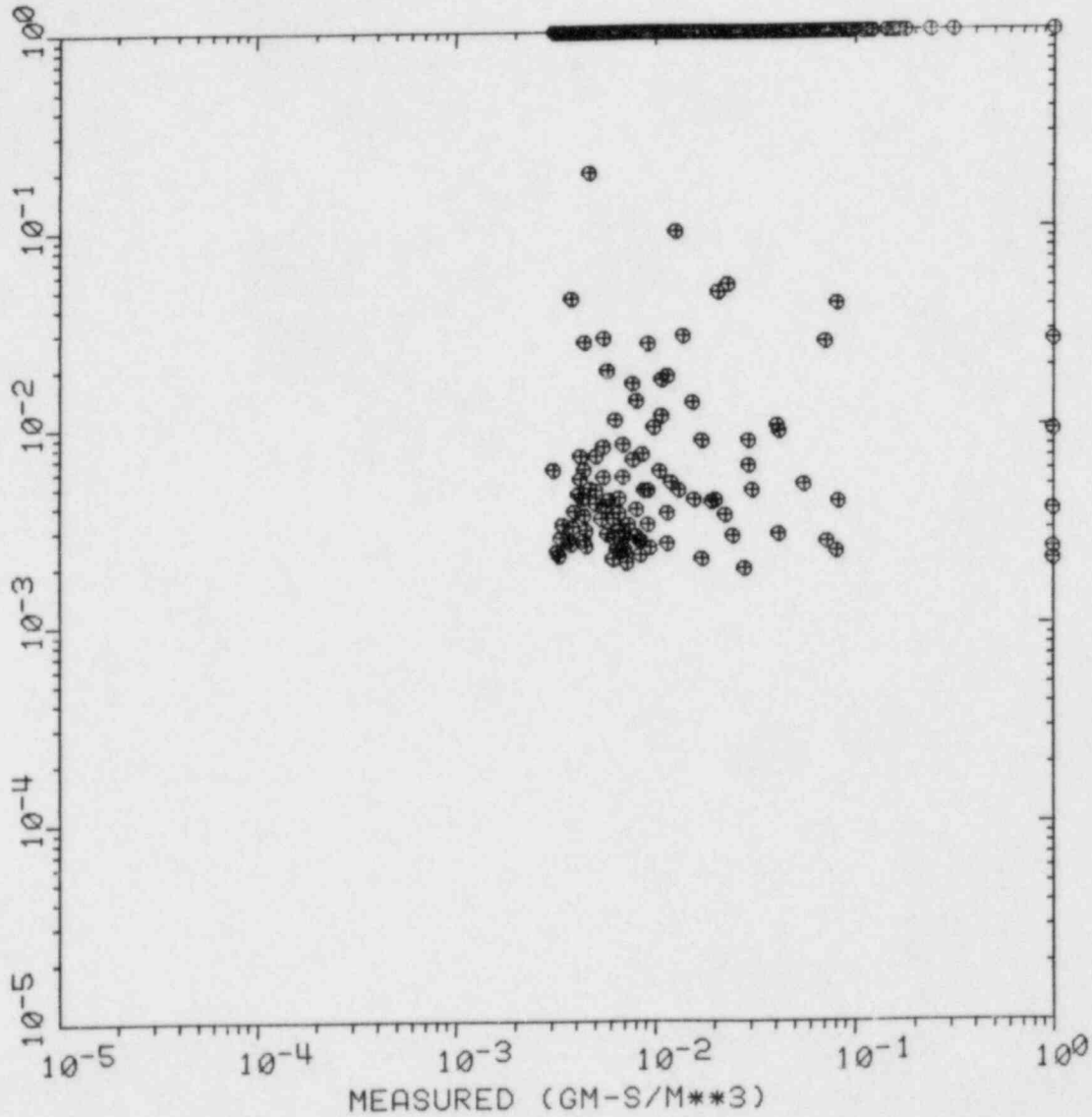


Fig. A-6 Modeled versus observed concentrations for small grid, test 2

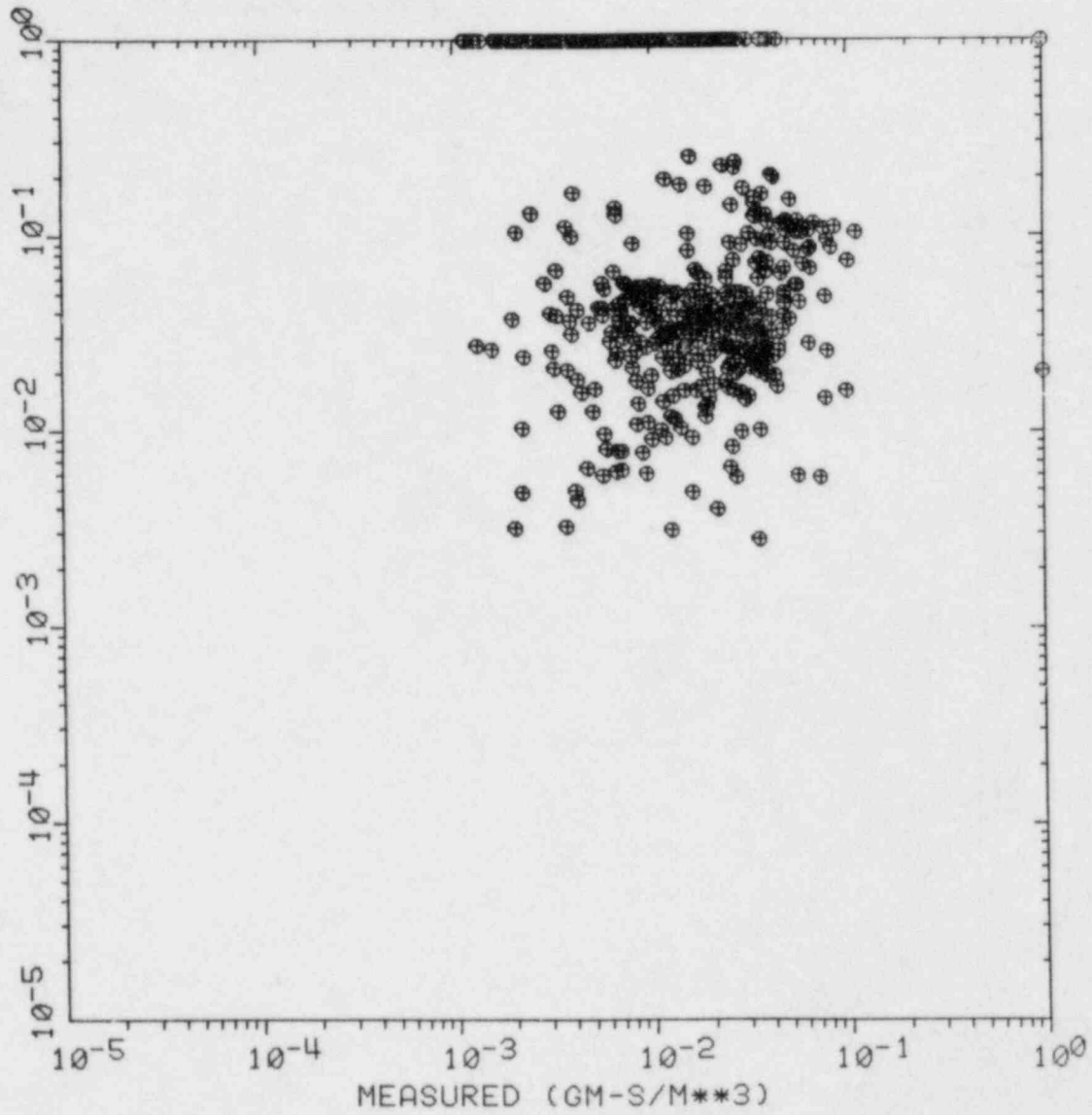


Fig. A-7 Modeled versus observed concentrations for small grid, test 3

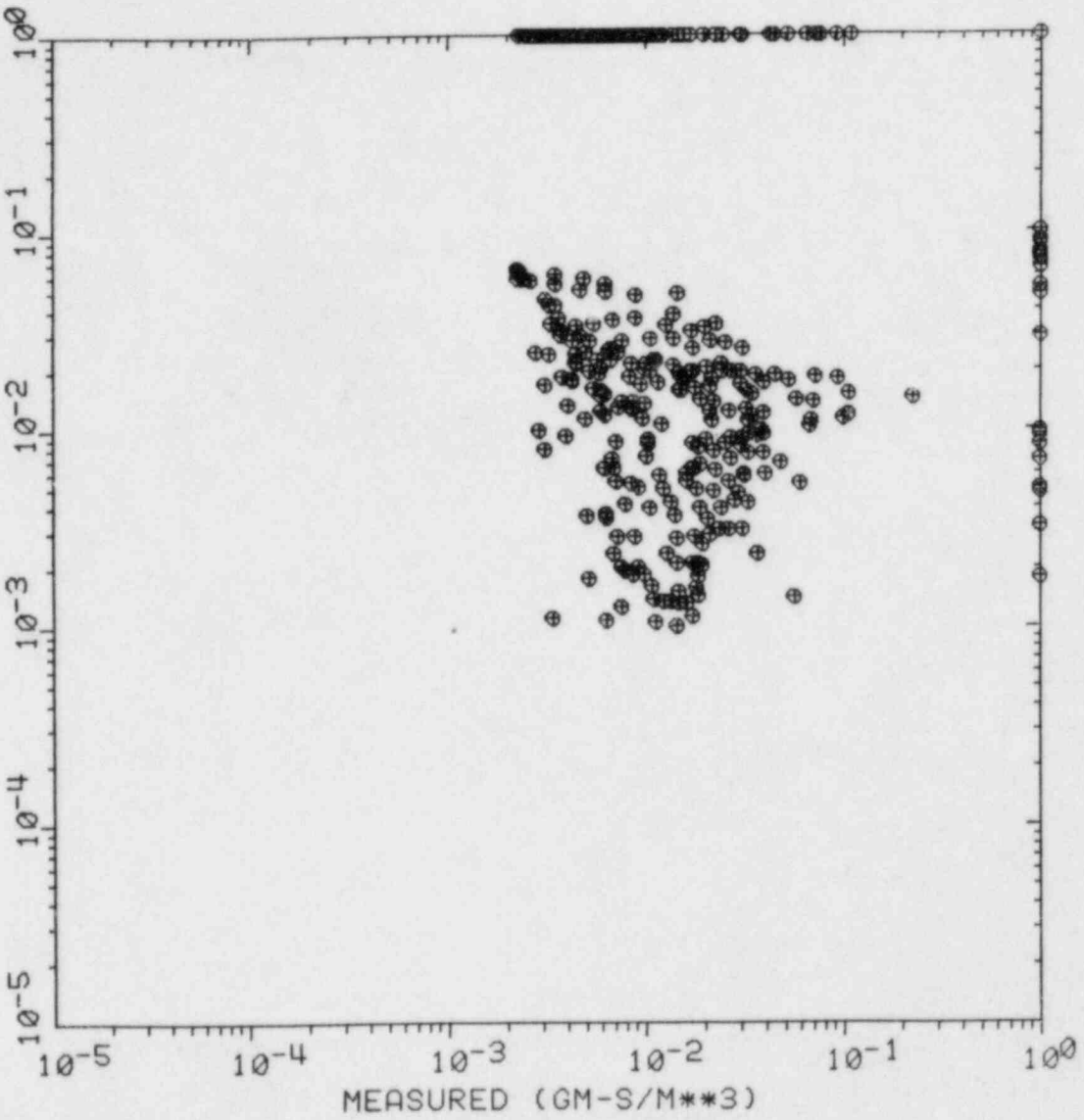


Fig. A-8 Modeled versus observed concentrations for small grid, test 4

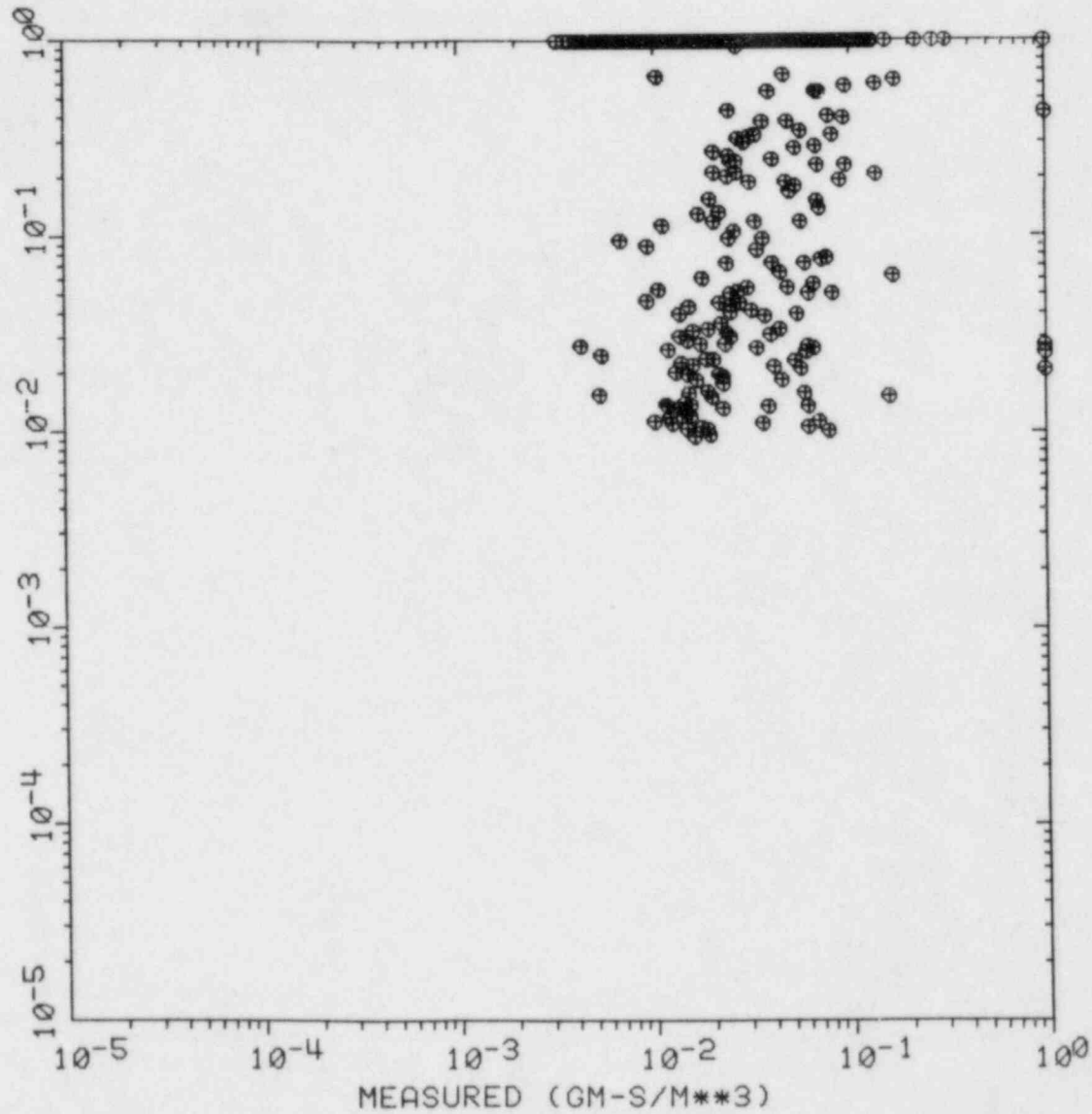


Fig. A-9 Modeled versus observed concentrations for small grid, test 5

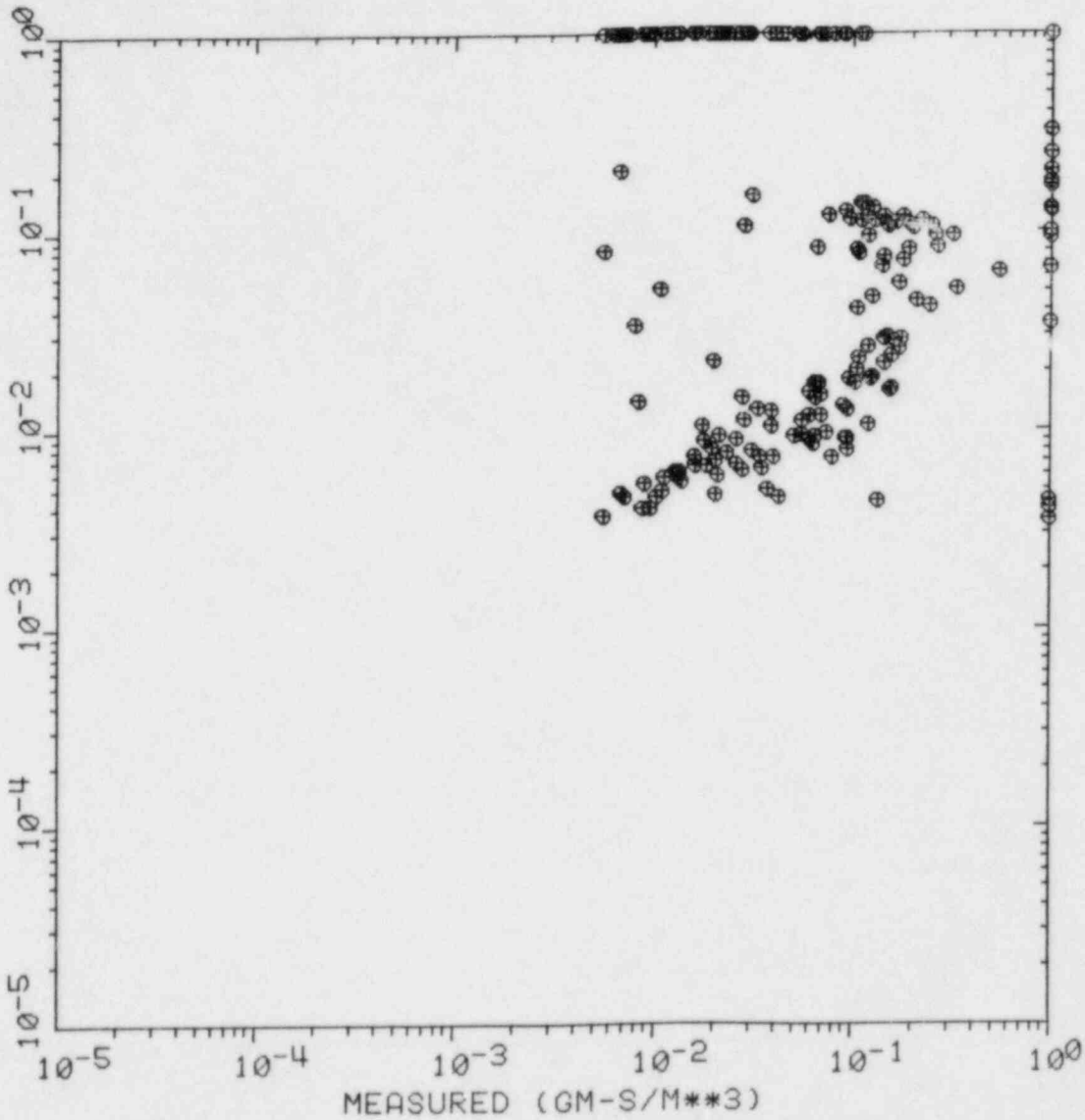


Fig. A-10 Modeled versus observed concentrations for small grid, test 6

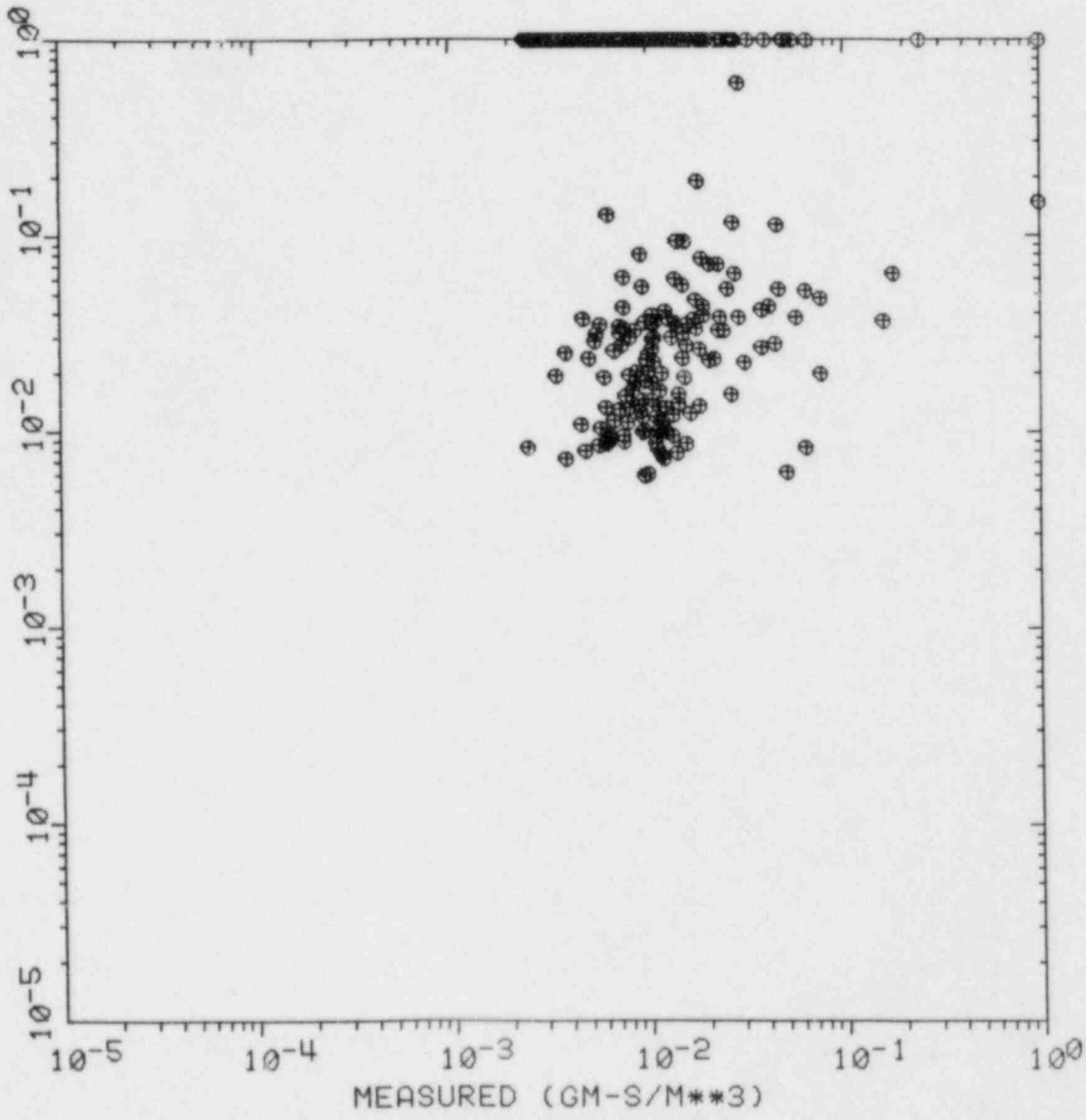


Fig. A-11 Modeled versus observed concentrations for small grid, test 7

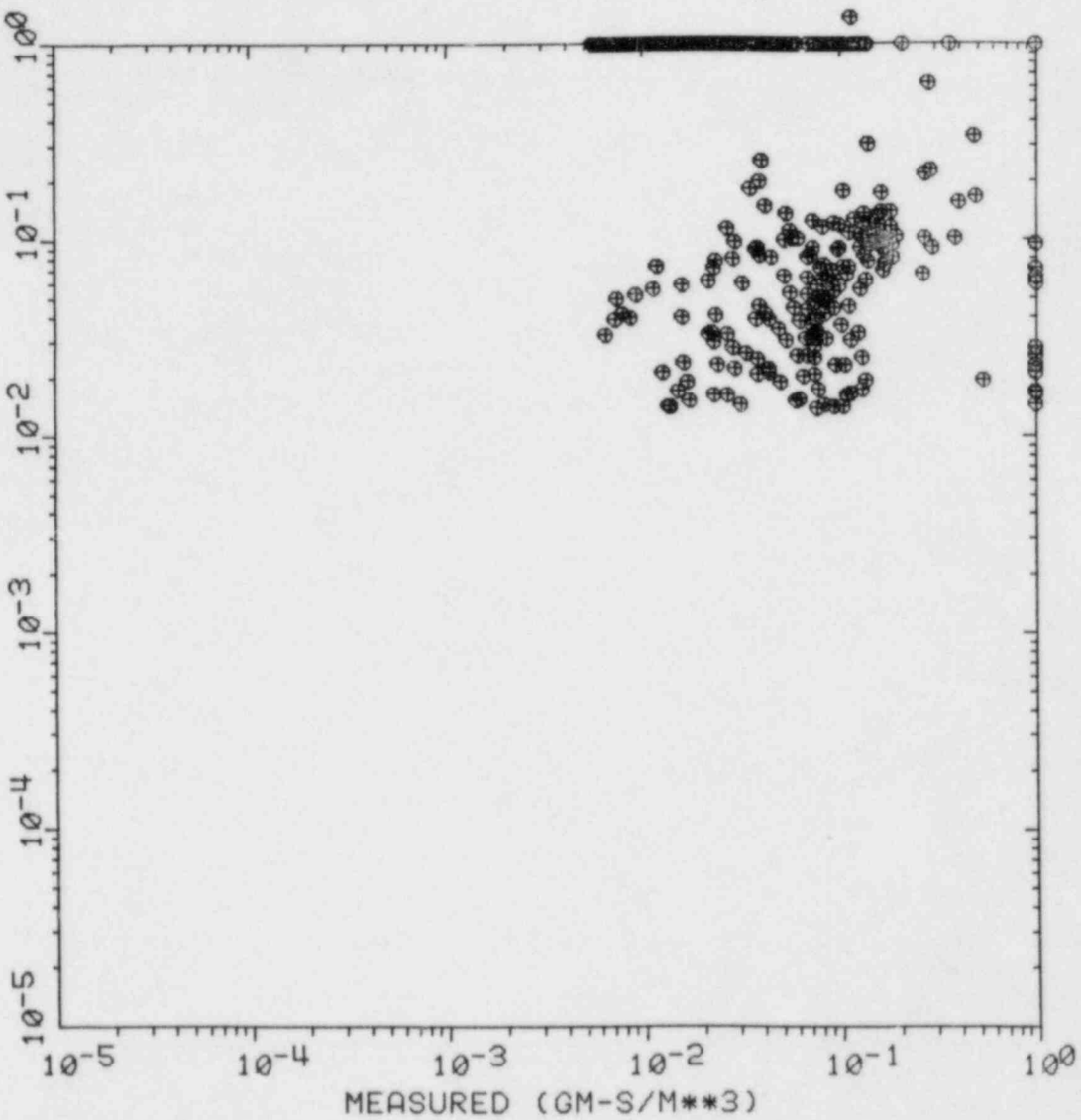


Fig. A-12 Modeled versus observed concentrations for small grid, test 8

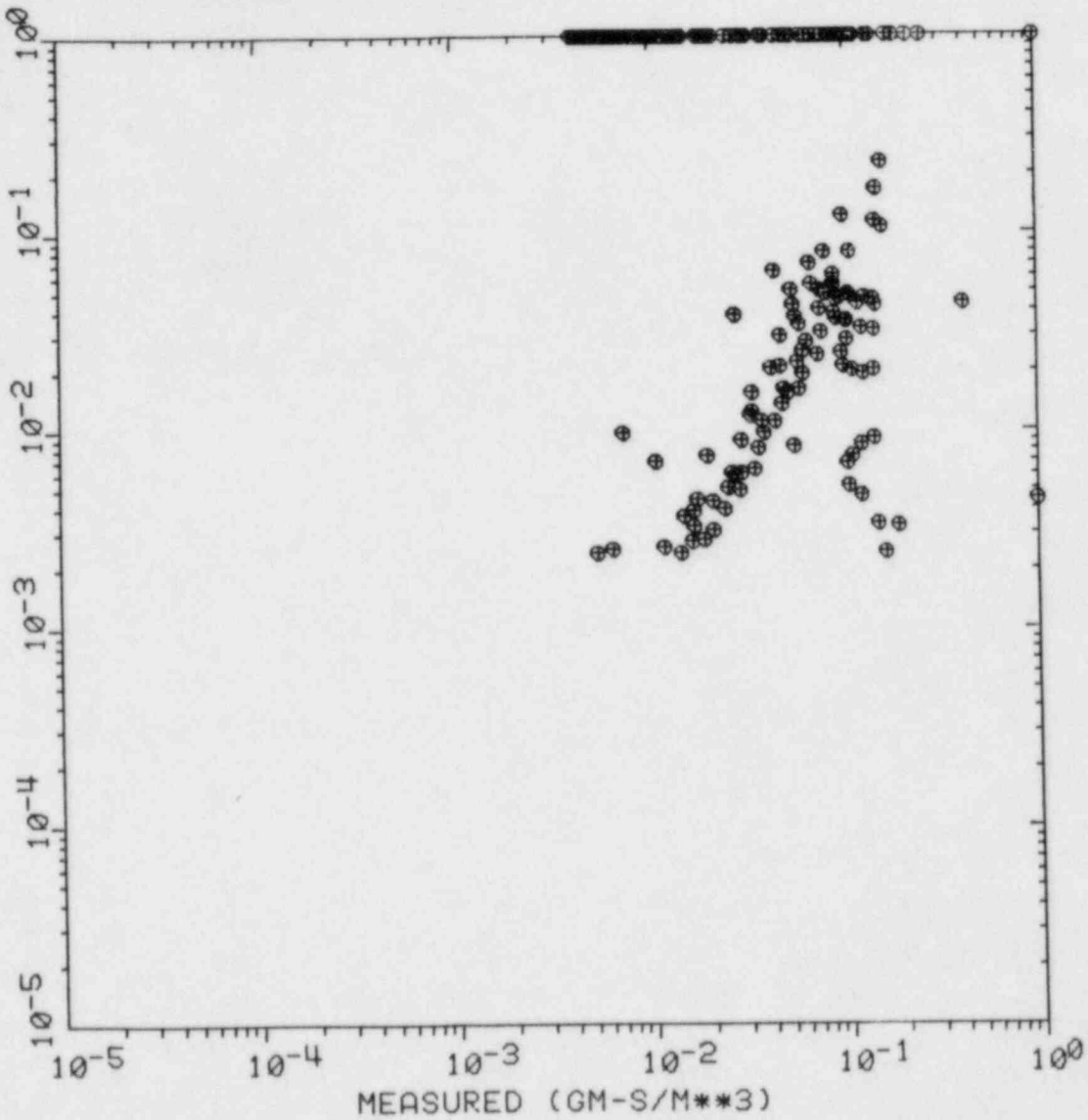


Fig. A-13 Modeled versus observed concentrations for small grid, test 9

## APPENDIX B

Methods used to interpolate concentration data for comparisons.

In order to perform comparisons between modeled and observed tracer behaviors, it is desirable to specify either an area weighting technique for the concentration observations (which are not always evenly spaced throughout the grid) or to specify a spatial interpolation technique to place the observed concentrations onto a uniform computational array. A spatial interpolation technique was utilized. Once the technique had been adopted the comparisons of calculations and observations were straightforward.

An interpolation grid was first initialized. Then sample data points were mapped onto the interpolation grid at points corresponding to their grid position. An indicator was set at each sample data point; at no time in the scheme was an actual data value altered. The boundary of the scheme was the outer row of sample data in each direction. The boundaries were filled by a simple linear interpolation or extrapolation from actual sample data along the boundary. These points were held fixed for the remainder of the scheme.

The interior of the interpolation grid was filled by a five point star weighting average relaxation scheme. The depiction below illustrates this scheme. The ij subscripts refer to grid location at *; the t superscript refers to timestep. The (i,j) point is being averaged. More detailed discussions on this technique may be found in customary numerical analysis texts under the heading of relaxation methods. The method may slightly tend to propagate values outward from an observed data point into areas where no sample was collected. This tendency should not be a problem in this data set.

$$
\begin{array}{ccc}
 & *\ {}^{t}_{ij+1} & \\
*\ {}^{t+1}_{i-1j} & *\ {}^{t}_{ij} & *\ {}^{t}_{i+1j} \\
 & *\ {}^{t+1}_{ij-1} &
\end{array}
$$

The value at point (i,j) always falls between the minimum and maximum of the bounding values on the star. Computational iterations through the field were made until values at all points converged to within a preselected residual. Typically, 40 passes were required for the small grid while 10 passes were enough on the large grid.

NRC FORM 335 (2-84) NRCM 1102, 3201, 3202

U.S. NUCLEAR REGULATORY COMMISSION

# BIBLIOGRAPHIC DATA SHEET

SEE INSTRUCTIONS ON THE REVERSE

1. REPORT NUMBER (Assigned by NRC, add Vol. No., if any)
NUREG/CR-3488
Vol. 3

2. TITLE AND SUBTITLE
Idaho Field Experiment 1981
Volume 3: Comparison of Trajectories, Concentration Patterns and MESODIF Model Calculations

3. LEAVE BLANK

4. DATE REPORT COMPLETED
MONTH: February YEAR: 1985

5. AUTHOR(S)
G.E. Start, J.H. Cate, J.F. Sagendorf, G.R. Ackermann, C.R. Dickson, N.H. Nukari, L.G. Thorngren

6. DATE REPORT ISSUED
MONTH: February YEAR: 1985

7. PERFORMING ORGANIZATION NAME AND MAILING ADDRESS (Include Zip Code)
Air Resources Laboratories
Field Research Division
National Oceanic and Atmospheric Administration
Idaho Falls, ID 83401

8. PROJECT/TASK/WORK UNIT NUMBER

9. FIN OR GRANT NUMBER
B5690

10. SPONSORING ORGANIZATION NAME AND MAILING ADDRESS (Include Zip Code)
Division of Radiation Programs and Earth Sciences
Office of Nuclear Regulatory Research
U.S. Nuclear Regulatory Commission
Washington, DC 20555

11a. TYPE OF REPORT
Technical

b. PERIOD COVERED (Inclusive dates)

12. SUPPLEMENTARY NOTES

13. ABSTRACT (200 words or less)

The 1981 Idaho Field Experiment was conducted in southeastern Idaho over the Upper Snake River Plain. Nine test-day case studies were measured between July 15 and 30, 1981. Eight-hour releases of $SF_6$ gaseous tracer were made from 45 m above the ground. Tracer was sampled hourly, for 12 sequential hours at about 100 locations within an area 24 km square. Also, a single total integrated sample of about 30 hours duration was collected at approximately 100 sites within an area 48 by 72 km (using 6 km spacings). Extensive tower profiles of meteorology at the release point were collected. RAWINSONDES, RABALS and PIBALS were collected at 3 to 5 sites. Horizontal, low-altitude winds were monitored using the INEL MESONET. $SF_6$ tracer plumes were marked with co-located oil fog releases and bi-hourly sequential launches of tetroon pairs. Aerial LIDAR observations of the oil fog plume and airborne samples of $SF_6$ were collected. High altitude aerial photographs of daytime plumes were also collected. The Idaho Field Experiment is reported in three volumes. Volume 3 contains descriptions of the nine intensive measurement days. General meteorological conditions are described, trajectories and their relationships to analyses of gaseous tracer data are discussed, and overviews of test day cases are presented. Calculations using the ARLFRD MESODIF model are included and related to the gaseous tracer data. Finally, a summary and a list of recommendations are presented.

14. DOCUMENT ANALYSIS - a. KEYWORDS/DESCRIPTORS
atmospheric dispersion
gaseous tracers
LIDAR
meteorology
model validation
plume trajectories
tetroons

b. IDENTIFIERS/OPEN ENDED TERMS

15. AVAILABILITY STATEMENT
Unlimited

16. SECURITY CLASSIFICATION
(This page) Unclassified
(This report) Unclassified

17. NUMBER OF PAGES

18. PRICE

UNITED STATES
NUCLEAR REGULATORY COMMISSION
WASHINGTON, D.C. 20555